


JUNE 23 2023

Acoustics of thermoviscous fluids: The Kirchhoff–Helmholtz representation in generalized form

C. L. Morfey; M. C. M. Wright 



J Acoust Soc Am 153, 3447 (2023)

<https://doi.org/10.1121/10.0019801>



View
Online



Export
Citation

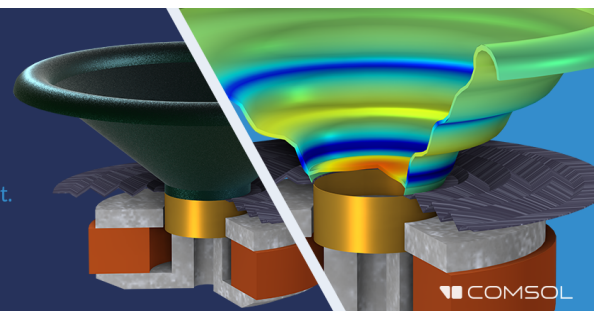
CrossMark

06 July 2023 14:28:43

Take the Lead in Acoustics

The ability to account for coupled physics phenomena lets you predict, optimize, and virtually test a design under real-world conditions – even before a first prototype is built.

» Learn more about COMSOL Multiphysics®



COMSOL

Acoustics of thermoviscous fluids: The Kirchhoff–Helmholtz representation in generalized form

C. L. Morfey¹ and M. C. M. Wright^{2,a)} 

¹School of Engineering, University of Leicester, Leicester LE1 7RH, United Kingdom

²Institute of Sound and Vibration Research, University of Southampton, Southampton SO17 1BJ, United Kingdom

ABSTRACT:

The Kirchhoff–Helmholtz representation of linear acoustics is generalized to thermoviscous fluids, by deriving separate bounded-region equations for the acoustic, entropy, and vorticity modes in a uniform fluid at rest. For the acoustic and entropy modes we introduce modal variables in terms of pressure and entropy perturbations, and develop asymptotic approximations to the mode equations that are valid to specified orders in two thermoviscous parameters. The introduction of spatial windowing for the mode variables leads to surface source and dipole distributions as a way of representing boundary conditions for each mode. For the acoustic mode the boundary source distribution is expressible in terms of the fluid normal velocity, the normal heat flux, and the vector $\boldsymbol{\omega} \times \hat{\mathbf{n}}$, where $\boldsymbol{\omega}$ is the vorticity on the boundary and $\hat{\mathbf{n}}$ is the unit normal; only the first of these is present in the usual lossless-fluid version of the Kirchhoff–Helmholtz representation. Use of the generalized thermoviscous representation to project exterior sound fields from surface data, where the data may contain contributions from all three linear modes, is shown to be robust to cross-modal contamination. The asymptotic limitations of the thermoviscous modal equations are discussed in an appendix. © 2023 Author(s). All article content, except where otherwise noted, is licensed under a Creative Commons Attribution (CC BY) license (<http://creativecommons.org/licenses/by/4.0/>).

<https://doi.org/10.1121/10.0019801>

(Received 27 September 2022; revised 12 May 2023; accepted 5 June 2023; published online 23 June 2023)

[Editor: Andi Petculescu]

Pages: 3447–3468

NOMENCLATURE

a	Thermal expansion parameter $a = \alpha/\rho c_p$	k_a, k_h, k_w	Characteristic wavenumbers for acoustic, entropy and vorticity modes
A, B	Dimensionless thermodynamic properties $A = \alpha T$ and $B = \alpha c^2/c_p$	K_a, K_h, K_w	Propagation wavenumbers for acoustic, entropy and vorticity modes; $K_l = \sqrt{k_l^2 - m^2}$ for $l = a, h, w$
c, c_0	Sound speed $c = (\partial p/\partial \rho)_s^{1/2}$, unperturbed value	$\mathcal{L}_a, \mathcal{L}_h$	Time-domain operators describing propagation of the acoustic and entropy modes in the absence of volume sources
c_p, c_v	Constant-pressure and constant-volume specific heats	m	Wavenumber in x direction (Sec. III G 2); axial wavenumber in cylindrical coordinates
$f(\mathbf{x}, t)$	Indicator function, positive in \mathcal{V} and negative in $\bar{\mathcal{V}}$, with $ \nabla f = 1$ on $\bar{\mathcal{S}}$	$\hat{\mathbf{n}}$	Unit vector normal to surface $\bar{\mathcal{S}}$, pointing outward from excluded region $\bar{\mathcal{V}}$
\mathbf{g}	Fluctuating body force distribution per unit mass	p, p'	Thermodynamic pressure and its perturbation relative to the uniform reference state $p' = p - p_0$
g_∞, g_N	Frequency-domain Green's functions (free-field, Neumann)	P	Non-dimensional pressure fluctuation $P = p'/\rho_0 c_0^2$
g_a, g_h	Frequency-domain Green's functions for the acoustic and entropy modes	P_a, P_h	Acoustic-mode and entropy-mode components of P in source-free regions
\mathcal{G}	Time-domain dimensionless heat-conduction operator $\mathcal{G} = t_\kappa \partial/\partial t = (\chi/c^2) \partial/\partial t$	\hat{P}_a, \hat{P}_h	Complex amplitudes of P_a and P_h in the frequency domain
$H(f)$	Heaviside (unit step) function acting as a spatial window	\tilde{P}_a	Dimensionless acoustic-mode pressure reconstructed from data on $r = r_0$ (Sec. VIIC)
$H_n^{(1)}(\xi)$	Hankel function of the first kind $H_n^{(1)}(\xi) = J_n(\xi) + iY_n(\xi)$	Pr	Shear Prandtl number $\text{Pr} = \nu/\chi$
i	Imaginary unit	\mathbf{q}, q_i	Heat flux vector, cartesian components ($i = 1, 2, 3$)
$J_n(\xi)$	Bessel function of the first kind of order n		
k_0	Lossless acoustic wavenumber ω/c_0		

^{a)}Electronic mail: mcmw@isvr.soton.ac.uk

q_n	Heat flux normal to boundary	$\tilde{\varepsilon}_\kappa = t_\kappa/\tilde{\tau} = \chi/c^2\tilde{\tau}$	and	$\tilde{\varepsilon}_L = t_L/\tilde{\tau}$
r	Radial coordinate in cylindrical coordinates	$= \mu_L/\rho c^2\tilde{\tau}$		
\mathcal{R}	Time-domain dimensionless viscous operator $\mathcal{R} = t_L\partial/\partial t = (\mu_L/\rho c^2)\partial/\partial t$	$\tilde{\varepsilon}$	$\max(\tilde{\varepsilon}_\kappa, \tilde{\varepsilon}_L)$	
s, s'	Specific entropy and its perturbation relative to the uniform reference state $s' = s - s_0$	ζ	Curl of vorticity $\zeta = \text{curl } \omega$	
S	Non-dimensional entropy perturbation $S = s'/c_{p0}$	ζ_n	Normal component of ζ at a boundary	
S_a, S_h	Acoustic-mode and entropy-mode components of S in source-free regions	θ	Azimuthal coordinate in cylindrical coordinates	
\hat{S}_a, \hat{S}_h	Complex amplitudes of S_a and S_h in the frequency domain	$i = a, h, w$	Generic label for linear modes (acoustic, entropy, vorticity)	
\bar{S}	Fixed surface separating excluded region $\bar{\mathcal{V}}$ from region \mathcal{V} , defined by $f(\mathbf{x}) = 0$	κ	Thermal conductivity	
t	Time	λ_a, λ_h	Polarization coefficients $\lambda_a = \hat{S}_a/\hat{P}_a$, $\lambda_h = \hat{P}_h/\hat{S}_h$ for $e^{-i\omega t}$ time dependence	
t_κ, t_L	Thermal diffusion and longitudinal viscosity time scales for fluid $t_\kappa = \kappa/\rho c_p c^2 = \chi/c^2$ and $t_L = \mu_L/\rho c^2$	$\tilde{\lambda}_a, \tilde{\lambda}_h$	Time-domain operators corresponding to λ_a and λ_h in the frequency domain	
T, T'	Thermodynamic temperature and its perturbation relative to the uniform reference state $T' = T - T_0$	$\Lambda_{aa}, \Lambda_{ah}, \Lambda_{aw}$	Coefficients that define the contribution of each mode to the projected sound field, Eq. (92)	
\mathbf{u}, u_i	Fluid velocity, cartesian components ($i = 1, 2, 3$)	μ	Shear viscosity	
$\mathbf{u}_a, \mathbf{u}_h, \mathbf{u}_w$	Modal components of fluid velocity ($\mathbf{u}_a = \nabla\phi_a$, $\mathbf{u}_h = \nabla\phi_h$, $\mathbf{u}_w = \text{curl } \mathbf{w}$)	μ_B	Bulk viscosity	
u_n	Normal component of \mathbf{u} at boundary	μ_L	Longitudinal viscosity $\mu_L = \mu_B + \frac{4}{3}\mu$	
\mathcal{V}	Region of interest where the linearized equations of fluid motion apply	ν	Kinematic viscosity $\nu = \mu/\rho$	
$\bar{\mathcal{V}}$	Excluded region, adjacent to \mathcal{V}	ξ	Source radius	
\mathbf{w}	Vector potential for the vorticity mode	ρ, ρ'	Density and its perturbation relative to the uniform reference state $\rho' = \rho - \rho_0$	
x	Axial coordinate in cylindrical coordinates	σ	Time-varying rate of external heat input per unit volume	
\mathbf{x}, x_i	Position vector, cartesian components ($i = 1, 2, 3$)	$\tilde{\tau}$	Typical time scale of an unsteady flow perturbation	
X_a, X_h	Acoustic and entropy mode dimensionless squared wavenumbers (inverse eigenvalues)	ϕ_a, ϕ_h	Velocity potential contributions due to acoustic and entropy modes in source-free regions	
Y	Longitudinal Prandtl number $Y = c_{p0} \mu_L/\kappa = t_L/t_\kappa = \varepsilon_L/\varepsilon_\kappa = \tilde{\varepsilon}_L/\tilde{\varepsilon}_\kappa$	Φ	Approximate mode variable for entropy mode (dimensionless)	
α	Thermal expansivity $\alpha = \rho(\partial\rho^{-1}/\partial T)_p$	χ	Thermal diffusivity $\chi = \kappa/\rho c_p$	
β	Non-dimensional wavenumber $\beta = \sqrt{1 - (m/k_0)^2}$ (Sec. III G 2)	$\psi(\mathbf{x}, t)$	An arbitrary continuous function	
γ	Ratio of specific heats $\gamma = c_p/c_v$	Ψ	Approximate mode variable for acoustic mode (dimensionless)	
Γ_a, Γ_h	Forcing terms to account for the presence of volume sources	ω	Angular frequency	
Γ_Ψ, Γ_Φ	Source distributions for the windowed mode variables Ψ_H, Φ_H	ω	Vorticity $\omega = \text{curl } \mathbf{u}$	
$\delta(f)$	Dirac delta function	\sim	Varies asymptotically as	
$\Delta; \Delta_a, \Delta_h$	Relative error in asymptotic modal approximations; acoustic and entropy mode values of Δ	\simeq	Asymptotically equals	
$\varepsilon_\kappa, \varepsilon_L$	Thermal-diffusion-scaled and longitudinal-viscosity-scaled frequency parameters $\varepsilon_\kappa = \omega t_\kappa = \omega\chi/c^2$ and $\varepsilon_L = \omega t_L = \omega\mu_L/\rho c^2$			
ε	$\max(\varepsilon_\kappa, \varepsilon_L)$			
$\tilde{\varepsilon}_\kappa, \tilde{\varepsilon}_L$	Thermal-diffusion-scaled and longitudinal-viscosity-scaled time-domain parameters			

I. INTRODUCTION

Linear perturbations to the state of a stationary initially-uniform compressible fluid possessing both viscosity and heat conduction can travel in three distinct modes of motion: the acoustic mode, which propagates by wave motion, and the entropy and vorticity modes, which diffuse through heat conduction and viscosity, respectively (Kovácszay, 1953). The propagation of these three modes in volume-source-free regions away from boundaries is described in the textbook by Pierce (1994). In the present article we present wave and diffusion equations for these three modes, including the effects of external volume sources. The external sources considered are a distributed heating rate $\sigma(\mathbf{x}, t)$ per unit volume as in Pierce (1985), and a distributed body force $\mathbf{g}(\mathbf{x}, t)$

per unit mass. In general, each of these inputs generates a response in the acoustic and entropy modes, while the applied force distribution drives the vorticity mode as well. The treatment here follows the early work by [Pierce \(1985\)](#) on thermoacoustic sound generation by external sources and extends it to bounded regions. For waves in isotropic heat-conducting elastic solids a corresponding set of linear modes exists, in which the diffusive vorticity mode is replaced by elastic shear waves ([Deresiewicz, 1957](#)); all the results of the present paper can be adapted to the solid case via a simple transformation, however, this is outside the scope of the present article.

The equations are presented to various orders of accuracy appropriate to the time scale of the forcing, with the form of the dependent variables for the acoustic and entropy modes changing according to the order chosen. In the frequency domain the relevant order parameters are $\varepsilon_\kappa = \omega\chi/c^2$ and $\varepsilon_L = \omega[\mu_B + \frac{4}{3}\mu]/\rho c^2$, where χ is the fluid thermal diffusivity, μ is the viscosity, and μ_B the bulk viscosity, while in the time domain they are $\tilde{\varepsilon}_\kappa = \tilde{\tau}^{-1}\chi/c^2$ and $\tilde{\varepsilon}_L = \tilde{\tau}^{-1}[\mu_B + \frac{4}{3}\mu]/\rho c^2$, where $\tilde{\tau}$ is a representative time scale of the perturbations.

In the case of the acoustic mode the results allow the extension of the Kirchhoff–Helmholtz representation, where domain boundaries are represented by monopole and dipole layers, to real fluids with viscosity and heat conduction. This representation of the sound field, expressible either in differential equation form (as here) or as a Green’s function solution for the acoustic variable, is usually restricted to ideal or lossless fluids ([Bruneau, 2006](#); [Morse and Ingård, 1968](#); [Temkin, 1981](#)). The textbook by [Pierce \(1994\)](#) provides a version [Eq. (10–6.7)], in integral form, in which effects of viscosity are included as an asymptotic approximation. Following Pierce, we avoid restricting the fluid to a perfect gas; instead, for equilibrium thermodynamic states the specific entropy can be any function $s(\rho, e)$ of the fluid density and specific internal energy. The resulting expressions are given in differential rather than integral form, to facilitate their use with tailored Green’s functions if required.

The generalized linear-mode theory developed here could be readily extended to describe nonlinear sound generation in thermoviscous media, as was first attempted for an ideal gas by [Chu and Kováznay \(1958\)](#). In anticipation of this the equations are given in the time domain, rather than the frequency domain.

II. THEORETICAL BACKGROUND

There is extensive literature dealing with the fundamental acoustics of thermoviscous fluids, including liquids and gases. By way of orientation, some of the key references are reviewed below.

A. Boundary-driven linear sound fields

This category encompasses boundary-driven fields where thermoviscous effects are important, propagation in narrow ducts, and sound fields excited in small cavities;

external volume sources are generally absent in these situations. Close to solid boundaries, unsteady diffusion of vorticity and entropy from the boundary generates unsteady boundary layers that interact with the acoustic field. To describe this situation, different formulations of the linearized equations of motion for thermoviscous fluids have been adopted by different authors according to the application envisaged.

- (1) [Rayleigh \(1894\)](#) (Sec. 348) derived a fourth-order differential equation describing single-frequency temperature disturbances of small amplitude in an otherwise uniform thermoviscous fluid, whose equilibrium pressure and specific internal energy are functions $p(\rho, T)$, $e(\rho, T)$ of density and temperature. Rayleigh’s derivation extended an earlier study by [Kirchhoff \(1868\)](#) in which the fluid was assumed to be an ideal gas. Viscous stresses and heat conduction were assumed to obey the Navier–Stokes–Fourier equations in both studies, with bulk viscosity included by [Rayleigh \(1894\)](#).
- (2) [Bruneau et al. \(1989\)](#) derived a time-domain version of Rayleigh’s T' equation, similarly applicable to a general fluid, as a preliminary to discussing its entropy and acoustic mode solutions. For ideal-gas applications, the corresponding version of Rayleigh’s single-frequency equation was presented in the review paper by [Beltman \(1999\)](#).
- (3) It is not generally possible, in the time domain, to factorize the T' equation into separate differential equations of integer order, with one describing the acoustic mode and the other the entropy mode [the time-domain operator R in Eq. (10) of [Bruneau et al. \(1989\)](#) is not an integer-order differential operator, since it involves a square root]. The exception is the special case considered by [Trilling \(1955\)](#) in which the fluid’s thermal and viscous timescales coincide. However, approximate time-domain mode equations can be obtained when $(\tilde{\varepsilon}_L, \tilde{\varepsilon}_\kappa)$ are both small so that disturbance time scales are long compare with the thermal and viscous time scales ([Pierce, 1994](#)), and we shall pursue this approach in Sec. III.
- (4) The textbook by [Morse and Ingård \(1968, Sec. 6.4\)](#) derives separate linearized equations for T' and p' in a general thermoviscous fluid. Rather than seeking separate equations for the acoustic and entropy modes, they suggest solving the simultaneous (T', p') equations directly, alongside the vorticity mode equation. This approach has been widely followed in the photoacoustics and thermoacoustics literature ([Guiraud et al., 2019](#); [McDonald and Wetsel, 1978](#)).
- (5) The textbook by [Pierce \(1994\)](#) (Sec. 10–6) adopts the weakly thermoviscous approximation mentioned in (3) above in order to examine viscosity effects on sound radiation. The present paper extends Pierce’s approach to include fluid heat conduction, leading to a generalization of the Kirchhoff–Helmholtz relation that applies to thermoviscous fluids.

B. Sound radiation from volume source distributions

Although some acoustics textbooks, such as [Temkin \(1981\)](#) and [Howe \(1996\)](#), introduce external sources of heat and momentum into the linearized equations of acoustics, the resulting forced equations are normally restricted to ideal fluids lacking viscosity or heat conduction. The only two published discussions known to us that examine the excitation of linear modes in thermoviscous fluids by external volume sources, either in the form of an unsteady heat input or an unsteady body force distribution, are [Chu and Kovásznyai \(1958\)](#) and [Pierce \(1985\)](#). In both papers the authors assume boundaries to be absent. The authors also both introduce weakly thermoviscous approximations, but in different ways: Chu and Kovásznyai assume that all three modes share a single length scale \tilde{l} such that $\nu_0/\tilde{l}c_0 \ll 1$, where $\nu = \mu/\rho$ is the kinematic viscosity of the fluid, reflecting their interest in hot-wire measurements of turbulence in the presence of a mean flow. On the other hand, Pierce assumes that all three modes share a single time scale $\tilde{\tau}$, with $\nu_0/\tilde{\tau}c_0^2 \ll 1$. A secondary difference is that [Chu and Kovásznyai \(1958\)](#) follow [Trilling \(1955\)](#) in assuming the fluid to be an ideal gas with $Pr = 3/4$ and $\mu_B = 0$, whereas [Pierce \(1985\)](#) allows for a general fluid but with the extra requirements $\mu_B/\tilde{\tau}\rho_0c_0^2 \ll 1$ and $\chi_0/\tilde{\tau}c_0^2 \ll 1$.

In Sec. III of the present paper we follow [Pierce \(1985\)](#) in assuming a common time scale, and extend his analysis by (i) including boundaries and (ii) including body forces as well as unsteady heating. We shall also consider the excitation of all three linear modes, rather than the acoustic mode alone.

III. ACOUSTIC AND ENTROPY MODES IN BOUNDED FLUID REGIONS

A. Summary of basic equations

The equations of motion for a general fluid may be written in the form

$$\Theta = \frac{-1}{\rho} \frac{D\rho}{Dt}, \tag{1}$$

$$\frac{Du_j}{Dt} = g_j + \frac{1}{\rho} \left(\frac{\partial \tau_{ij}}{\partial x_i} - \frac{\partial p}{\partial x_j} \right), \tag{2}$$

$$\rho T \frac{Ds}{Dt} = \sigma - \frac{\partial q_i}{\partial x_i} + \tau_{ij} \frac{\partial u_j}{\partial x_i}. \tag{3}$$

Here, D/Dt denotes the material derivative, \mathbf{u} is the fluid velocity, and $\Theta = \text{div } \mathbf{u}$ is the dilatation rate. The thermodynamic properties (T, p, s) are equilibrium values; thus, symbol p denotes the thermodynamic pressure of the fluid $p(\rho, e) = -(\partial e / \partial \rho^{-1})_s$. The actual instantaneous pressure, p_{inst} , defined as the average compressive stress in three orthogonal directions, can differ from p as a result of non-equilibrium effects. This difference is included as an isotropic-stress term in the viscous stress τ_{ij} ; it is modelled in Eq. (4) below by introducing a bulk viscosity. The

external-forcing variables (σ, \mathbf{g}) are respectively the heat input rate per unit volume, and the applied force per unit mass of fluid.

For sufficiently small departures from local thermal equilibrium, according to the Navier–Stokes–Fourier model, the non-equilibrium stress components τ_{ij} and the heat flux q_i in Eq. (3) are linearly related to the fluid deformation rate and the temperature gradient, respectively, by

$$\tau_{ij} = \mu \left(\frac{\partial u_i}{\partial x_j} + \frac{\partial u_j}{\partial x_i} - \frac{2}{3} \Theta \delta_{ij} \right) + \mu_B \Theta \delta_{ij} \tag{4}$$

and

$$q_i = -\kappa \frac{\partial T}{\partial x_i}, \tag{5}$$

where κ is the thermal conductivity. In Eq. (2) the viscous force per unit volume is given by the divergence of τ_{ij} . For the special case of a fluid whose viscosity coefficients μ, μ_B are constant, Eq. (4) gives

$$\text{div } \boldsymbol{\tau} = -\mu \text{curl } \boldsymbol{\omega} - \mu_L \nabla \left(\frac{1}{\rho} \frac{D\rho}{Dt} \right). \tag{6}$$

Here $\boldsymbol{\omega} = \text{curl } \mathbf{u}$ is the vorticity, $\mu_L = [\mu_B + \frac{4}{3}\mu]$ is the longitudinal viscosity, and the continuity Eq. (1) has been used to substitute for Θ . A similar result can be derived for any fluid whose viscous stress is described by Eq. (4), provided one limits consideration to small perturbations about a uniform state of rest (denoted by subscript 0); omitting second-order terms then gives $\text{div } \boldsymbol{\tau} \simeq -\mu_0 \text{curl } \boldsymbol{\omega} - (\mu_{L0}/\rho_0) \nabla (\partial \rho' / \partial t)$.

Applying the same small-amplitude restriction to Eqs. (1)–(3) leads to the following set of linearized equations, in which primes denote fluid-property perturbations; the kinematic variables $\mathbf{u}, \Theta, \boldsymbol{\omega}$ are all perturbations about zero, since the undisturbed fluid is at rest, and are therefore left unprimed,

$$\Theta \simeq -\frac{1}{\rho_0} \frac{\partial \rho'}{\partial t}, \tag{7}$$

$$\rho_0 \frac{\partial \mathbf{u}}{\partial t} \simeq \rho_0 \mathbf{g} - \nabla p' - \mu_0 \text{curl } \boldsymbol{\omega} - \mu_{L0} \nabla \left(\frac{1}{\rho_0} \frac{\partial \rho'}{\partial t} \right), \tag{8}$$

$$\rho_0 T_0 \frac{\partial s'}{\partial t} \simeq \sigma + \kappa_0 \nabla^2 T'. \tag{9}$$

By combining the divergence of Eq. (8) with the time derivative of Eq. (7), one can eliminate the kinematic variables ($\mathbf{u}, \Theta, \boldsymbol{\omega}$) to concentrate on the acoustic and entropy modes; we will return to the vorticity mode in Sec. V. Coupled equations for the pressure and entropy perturbations can then be obtained by substituting ρ' in the resulting equation, and T' in Eq. (9), in terms of p' and s' by means of the linear approximations

$$\frac{1}{\rho_0} \rho' \simeq \left(\frac{1}{\rho c^2} \right)_0 p' - \left(\frac{\alpha T}{c_p} \right)_0 s' \tag{10}$$

and

$$\frac{1}{T_0} T' \simeq \left(\frac{1}{c_p}\right)_0 s' + \left(\frac{\alpha}{\rho c_p}\right)_0 p', \quad (11)$$

where α is the fluid's thermal expansivity. The two equations obtained in this way are expressed below in terms of the non-dimensional perturbation variables $P = p'/\rho_0 c_0^2$ and $S = s'/c_{p0}$. Zero subscripts are henceforth dropped on the understanding that linear approximations are being used throughout, and we introduce non-dimensional coefficients $A = \alpha T$ and $B = \alpha c^2/c_p$; the product $AB = \gamma - 1$ [Pierce (1994), Eqs. (1–9.9)], where γ is the ratio of specific heats, and for the special case of a dilute gas, $A = 1$ and $B = \gamma - 1$. We thus write

$$\frac{\partial^2 P}{\partial t^2} - A \frac{\partial^2 S}{\partial t^2} - c^2 \nabla^2 [P + \mathcal{R}(P - AS)] = -\text{div } \mathbf{g}, \quad (12)$$

$$\frac{\partial S}{\partial t} - \chi \nabla^2 (BP + S) = \frac{\sigma}{\rho c_p T}, \quad (13)$$

where $\chi = \kappa/\rho c_p$ is the fluid's thermal diffusivity, and the dimensionless operator \mathcal{R} is defined as $t_L \partial/\partial t$, where $t_L = \mu_L/\rho c^2$ is the characteristic viscous time scale for the fluid. We also define its thermal-diffusion time scale $t_\kappa = \chi/c^2$ (Pierce, 1994), and note that Bruneau *et al.* (1989) and Bruneau (2006) instead use length scales given by $\ell_v = ct_L$ and $\ell_h = ct_\kappa$. The ratio of these two time scales t_L/t_κ is then the longitudinal Prandtl number $Y = c_p \mu_L/\kappa$.

Our goal, in what follows, is to convert these coupled equations in P and S into uncoupled equations in dependent variables that correspond closely to pressure and specific entropy fluctuations. The right-hand side of these equations will include volume sources arising from the presence of \mathbf{g} and σ on the right of Eqs. (12) and (13). We begin, following Pierce (1994), by obtaining dispersion relations for single-frequency propagation in free space and in the absence of \mathbf{g} and σ input terms. We subsequently use these relations to obtain time-domain equations that satisfy the governing equations with volume sources present.

B. Single-frequency free travelling waves

In a region free of volume sources, Eqs. (12) and (13) set the conditions under which freely propagating solutions proportional to $\exp[i(\mathbf{k}(\omega) \cdot \mathbf{x} - \omega t)]$ can exist. To explore these conditions, we write

$$X = \frac{|\mathbf{k}(\omega)|^2}{(\omega/c)^2}, \quad (14)$$

and replace the operators $(\nabla^2, \partial/\partial t, \mathcal{R})$ with $(-\omega^2 X/c^2, -i\omega, -i\varepsilon_L)$, respectively, where $\varepsilon_L = \omega t_L = \omega \mu_L/\rho c^2$ is a longitudinal-viscosity-scaled frequency parameter. We also define a thermal-diffusion-scaled frequency parameter $\varepsilon_\kappa = \omega t_\kappa = \omega \chi/c^2$. With $(\sigma, \mathbf{g}) = 0$, Eqs. (12) and (13) can then be expressed in matrix form as

$$\begin{bmatrix} -A(1 + i\varepsilon_L X) & 1 - (1 - i\varepsilon_L)X \\ 1 + i\varepsilon_\kappa X & i\varepsilon_\kappa B X \end{bmatrix} \begin{pmatrix} \hat{P} \\ \hat{S} \end{pmatrix} = \begin{pmatrix} 0 \\ 0 \end{pmatrix}, \quad (15)$$

where \hat{P} and \hat{S} are the complex amplitudes of the propagating normalized pressure and entropy disturbances. Equation (15) is equivalent to Eq. (10–3.5) of Pierce (1994).¹ This can be rewritten as a generalized eigenvalue problem

$$\begin{bmatrix} -iA\varepsilon_L & i\varepsilon_L - 1 \\ i\varepsilon_\kappa & iB\varepsilon_\kappa \end{bmatrix} \begin{pmatrix} \hat{P} \\ \hat{S} \end{pmatrix} = X^{-1} \begin{bmatrix} A & -1 \\ -1 & 0 \end{bmatrix} \begin{pmatrix} \hat{P} \\ \hat{S} \end{pmatrix} \quad (16)$$

whose eigenvectors, denoted $(\hat{P}_a, \hat{S}_a)^T$ and $(\hat{P}_h, \hat{S}_h)^T$, normalized so that $\hat{P} = \hat{P}_a + \hat{P}_h$ and $\hat{S} = \hat{S}_a + \hat{S}_h$, are the acoustic and entropy modes, respectively. These modes propagate with frequency-dependent wavenumbers $k_a(\omega)$ and $k_h(\omega)$, respectively, obtained from the eigenvalues

$$X_{a,h}^{-1} = -\frac{1}{2} [1 - i\varepsilon_L - i\gamma\varepsilon_\kappa \pm \sqrt{4(1 - \gamma i\varepsilon_L)i\varepsilon_\kappa + (1 - i\varepsilon_L - \gamma i\varepsilon_\kappa)^2}], \quad (17)$$

where the plus sign corresponds to the acoustic mode and the identity $AB = \gamma - 1$ has been used.

The modal dispersion relations obtained from Eq. (17) imply the existence of Helmholtz operators \mathcal{H}_a and \mathcal{H}_h that govern the propagation of time-harmonic disturbances in the absence of volume sources; on physical grounds we expect the effect of \mathcal{H}_a to be dominated by wave motion and that of \mathcal{H}_h by diffusion. The Helmholtz operators can be defined by writing $\mathcal{H}_a = \nabla^2 + k_a^2$ and $\mathcal{H}_h = \nabla^2 + k_h^2$ as in Pierce (1994), where k_a and k_h are the characteristic wavenumbers for the acoustic and entropy modes. We find, however, that writing $\mathcal{H}_a = X_a^{-1} \nabla^2 + (\omega/c_0)^2$ and $\mathcal{H}_h = X_h^{-1} \nabla^2 + (\omega/c_0)^2$ leads to more compact expressions in what follows.

The eigenvectors provide proportionality relations between \hat{P} and \hat{S} for each mode. For the acoustic mode the ratio \hat{S}_a/\hat{P}_a is $O(\varepsilon)$, where $\varepsilon = \max(\varepsilon_\kappa, \varepsilon_L)$. It is given to lowest order by

$$\frac{\hat{S}_a}{\hat{P}_a} = \lambda_a \simeq -i\varepsilon_\kappa B. \quad (18)$$

Likewise for the entropy mode, labelled with subscript h , the ratio \hat{P}_h/\hat{S}_h is given to lowest order by

$$\frac{\hat{P}_h}{\hat{S}_h} = \lambda_h \simeq -i(\varepsilon_L - \varepsilon_\kappa)A, \quad (19)$$

with $\hat{P}_a + \hat{P}_h = \hat{P}$ and $\hat{S}_a + \hat{S}_h = \hat{S}$. These relations can be inverted to give

$$\hat{P}_a = \frac{\hat{P} - \lambda_h \hat{S}}{1 - \lambda_a \lambda_h}, \quad \hat{S}_h = \frac{\hat{S} - \lambda_a \hat{P}}{1 - \lambda_a \lambda_h}. \quad (20)$$

Equations (18) and (19) are called polarization relations in Pierce (1994); his terminology will be adopted in what follows with λ_a, λ_h referred to as polarization coefficients. Higher-order approximations for λ_a, λ_h are presented in Appendix A, together with the corresponding values of

k_a^2, k_h^2 as well as X_a^{-1}, X_h^{-1} that determine the modal dispersion relations and hence the propagation operators.

Trilling (1955) and Chu and Kováczny (1958) restricted their analyses to fluids with $\mu_B = 0$ and shear Prandtl number $c_{p0}\mu/\kappa = 3/4$. For such a fluid (or any other fluid with longitudinal Prandtl number $Y = 1$) the thermal and viscous time scales coincide so that $\varepsilon_L = \varepsilon_\kappa = \varepsilon$. In this special case the polarization coefficients reduce to $\lambda_a = Bi\varepsilon/[(\gamma - 1)i\varepsilon - 1]$ and $\lambda_h = 0$, meaning that $\hat{P}_h = 0$ and $\hat{P} = \hat{P}_a$, so the entire pressure field can be obtained from the acoustic mode. The eigenvalues become $X_a^{-1} = 1 - \gamma i\varepsilon$ and $X_h^{-1} = -i\varepsilon$, making it possible to obtain exact time-domain operators from \mathcal{H}_a and \mathcal{H}_h . In what follows we will instead obtain approximate versions of these operators to any required order of accuracy for unrestricted values of Y , by truncating series expansions in $(-i\varepsilon_L, -i\varepsilon_L)$ of the dispersion relations (17) and the polarization coefficients.

C. Time-domain modal equations with volume sources: Asymptotic approximations for $\tilde{\varepsilon}_\kappa \ll 1$ or $(\tilde{\varepsilon}_\kappa, \tilde{\varepsilon}_L) \ll 1$

The foregoing results allow one to construct approximate time-domain equations for acoustic and entropy mode variables, denoted by $\Psi(\mathbf{x}, t)$ and $\Phi(\mathbf{x}, t)$, respectively, that are valid when $(\sigma, \mathbf{g}) \neq 0$. The modal variables Ψ and Φ are linear combinations of P and S ; by analogy with Eq. (20) the acoustic mode variable Ψ should ideally be based on $P - \tilde{\lambda}_h S$ in order to cancel any entropy-mode contribution, and likewise the entropy mode variable Φ should be based on $S - \tilde{\lambda}_a P$. Here, $(\tilde{\lambda}_a, \tilde{\lambda}_h)$ are differential operators in time t , corresponding to the frequency-domain coefficients (λ_a, λ_h) . Our approximate mode variables Ψ and Φ are formed by using approximate versions of these operators, as explained below. Note that the product $\lambda_a \lambda_h$ in the denominators of Eq. (20) is order ε^2 , so for time-domain applications in which an error of relative order $\tilde{\varepsilon}^2$ is acceptable the denominator can be replaced by 1.

For this purpose the time-domain parameter $\tilde{\varepsilon}_\kappa = t_\kappa/\tilde{\tau}$ is assumed to be much less than 1 where $\tilde{\tau}$ is a typical time scale of the unsteady flow perturbations, meaning that disturbances take place over time scales that are long compared to t_κ . The parameter $\tilde{\varepsilon}_L = t_L/\tilde{\tau}$ can be restricted or not, depending on the level of accuracy required. We note that $\tilde{\varepsilon}_\kappa$ in the time domain corresponds to ε_κ in the frequency domain, and $\tilde{\varepsilon}_L$ corresponds to ε_L .

The resulting modal equations will have the general form

$$\mathcal{L}_a \Psi = \Gamma_a \quad \text{and} \quad \mathcal{L}_h \Phi = \Gamma_h, \tag{21}$$

with the particular form depending on the order of accuracy required, where \mathcal{L}_a and \mathcal{L}_h are time-domain propagation operators corresponding to the frequency-domain operators \mathcal{H}_a and \mathcal{H}_h introduced in Sec. III B above.

The forcing terms Γ_a and Γ_h necessary to satisfy the governing equations with volume sources (to the required accuracy) can be inferred from the following exact

expressions for the Laplacians of P and S , obtained from Eqs. (12) and (13) with the aid of the thermodynamic relation $AB = \gamma - 1$,

$$(1 + \gamma\mathcal{R})c^2\nabla^2 P = \frac{\partial^2 P}{\partial t^2} + \frac{c^2}{\chi}A(\mathcal{R} - \mathcal{G})\frac{\partial S}{\partial t} + \text{div } \mathbf{g} - c^2A\mathcal{R}\frac{\sigma}{\kappa T}, \tag{22}$$

$$(1 + \gamma\mathcal{R})c^2\nabla^2 S = \frac{c^2}{\chi}[1 + \mathcal{R} + (\gamma - 1)\mathcal{G}]\frac{\partial S}{\partial t} - B\frac{\partial^2 P}{\partial t^2} - B\text{div } \mathbf{g} - c^2(1 + \mathcal{R})\frac{\sigma}{\kappa T}. \tag{23}$$

The conversion of frequency-domain factors to time-domain operators is achieved by reversing the replacements given before Eq. (15). We make use of operators $\mathcal{R} = t_L\partial/\partial t$ and $\mathcal{G} = t_\kappa\partial/\partial t$. For purposes of time-domain asymptotic scaling, we note that $\mathcal{R} \sim \tilde{\varepsilon}_L$ and $\mathcal{G} \sim \tilde{\varepsilon}_\kappa$.

For monatomic gases the viscous and thermal length scales are comparable and are related to the molecular mean free path; likewise, the viscous and thermal time scales (t_L, t_κ) are comparable and related to the mean time between molecular collisions. For polyatomic gases including air on the other hand, vibrational relaxation effects limit the Navier–Stokes bulk viscosity model to frequencies well below the lowest relaxation frequency; in this frequency range t_L can be much greater than t_κ . For moist air at standard atmospheric pressure, 20 °C, and 60% relative humidity the relaxation frequencies of the vibrational modes for oxygen and nitrogen molecules are $f_r(\text{O}_2) = 44$ kHz, $f_r(\text{N}_2) = 400$ Hz (Bass *et al.*, 1990). At 5 °C, and 10% relative humidity these fall to $f_r(\text{O}_2) = 800$ Hz, $f_r(\text{N}_2) = 32$ Hz. For frequencies $f \ll f_r(\text{N}_2)$, vibrational relaxation effects may be modelled by an effective bulk viscosity $\mu_{B,\text{eff}} \gg \mu_B$ to which nitrogen makes the major contribution (3 to 4 orders of magnitude greater than the μ_B due to rotational relaxation). At the other extreme, for sufficiently high frequencies the vibrational degrees of freedom are “frozen,” the bulk viscosity model becomes valid again, and the attenuation of sound in air is dominated by rotational relaxation plus viscosity and heat conduction: for example at 20 °C, 60% RH this occurs beyond about 125 kHz, and at 5 °C, 10% RH beyond about 15 kHz.

Equations for the acoustic and entropy modes in a relaxing gas can be developed in a similar manner to the thermoviscous-fluid equations presented here, but lie outside the scope of the present paper. Note that in order for continuum theory to be valid for gases, we require $\varepsilon_\kappa = \omega t_\kappa \ll 1$ (Greenspan, 1950, 1956).

We illustrate the derivation of forced time-domain modal equations by means of two examples before presenting the full results.

1. Example 1: Entropy mode equation with $(\tilde{\varepsilon}_L, \tilde{\varepsilon}_\kappa) \ll 1$ and relative error $\Delta = \mathcal{O}(\tilde{\varepsilon})$

This example describes the derivation of the forced entropy-mode equation in row 4 of Table I below. Instead of

TABLE I. Time domain equations for free and forced linear modes in a viscous heat conducting fluid, valid throughout fluid region \mathcal{V} . Here, and in Table II, a single asterisk (*) after an equation means that it is asymptotically correct to the specified order in the limit $\tilde{\epsilon}_\kappa \ll 1$. A double asterisk (**) identifies equations that require both $\tilde{\epsilon}_L \ll 1$ and $\tilde{\epsilon}_\kappa \ll 1$.

Case	Mode variable ^a	Mode equation (unforced)	Volume forcing terms
1	Arbitrary $\tilde{\epsilon}_L$; acoustic mode, $\Delta = O(\tilde{\epsilon}_\kappa)$	$\Psi = (1 + \mathcal{R})^3 P - A[(1 + \mathcal{R})^2 \mathcal{R} - (1 + \gamma \mathcal{R}) \mathcal{G}] S$	*
2	Arbitrary $\tilde{\epsilon}_L$; entropy mode, $\Delta = O(\tilde{\epsilon}_\kappa)$	$\Phi = S$	*
3	$(\tilde{\epsilon}_L, \tilde{\epsilon}_\kappa) \ll 1$; acoustic mode, $\Delta = O(\tilde{\epsilon})$	$\Psi = P - A(\mathcal{R} - \mathcal{G}) S$	**
4	$(\tilde{\epsilon}_L, \tilde{\epsilon}_\kappa) \ll 1$; entropy mode, $\Delta = O(\tilde{\epsilon})$	$\Phi = S$	**
5	$(\tilde{\epsilon}_L, \tilde{\epsilon}_\kappa) \ll 1$; acoustic mode, $\Delta = O(\tilde{\epsilon}^2)$	$\Psi = P - A(\mathcal{R} - \mathcal{G})[1 - \mathcal{R} + (2 - \gamma) \mathcal{G}] S$	**
6	$(\tilde{\epsilon}_L, \tilde{\epsilon}_\kappa) \ll 1$; entropy mode, $\Delta = O(\tilde{\epsilon}^2)$	$\Phi = S - B \mathcal{G} P$	**

^aThe (Ψ, Φ) definitions vary according to the level of approximation being aimed at. In each case, the number of terms retained in Ψ or Φ is the minimum required for the governing linear mode equation to be asymptotically valid to the stated accuracy.

^bThe \mathcal{G} term in the operator is not required for $\Delta = O(\tilde{\epsilon}_\kappa)$ locally, but allows for long-range attenuation by heat conduction. In the corresponding row of Table II, it is omitted.
^cThe \mathcal{R} and \mathcal{G} terms in the operator are not required for $\Delta = O(\tilde{\epsilon})$ locally, but they allow for long-range attenuation by viscosity and heat conduction. In row 3 of Table II they are omitted. In the special case $Y = \tilde{\epsilon}_L / \tilde{\epsilon}_\kappa = 1$, the unforced equations in rows 3 and 5 coincide, with $\Psi = P$ and $\Delta = O(\tilde{\epsilon}^2)$; see Appendix B, Eq. (B8).

defining the entropy mode variable as $\Phi = S - \tilde{\lambda}_a P$, we note from Eq. (A4) that to the required order of accuracy $\tilde{\lambda}_a$ can be neglected, leaving the approximate entropy-mode variable $\Phi = S$.

The dispersion relation for the entropy mode is given by Eq. (A12); at the required order of accuracy, it reduces to $X_h^{-1} = -i\epsilon_\kappa$, meaning that the diffusion of an entropy disturbance would, in the absence of volume sources, be governed by

$$\mathcal{L}_h S = \left\{ \frac{\partial}{\partial t} - \chi \nabla^2 \right\} S \simeq 0. \tag{24}$$

With volume sources present, substituting Eq. (23) in Eq. (24) gives the exact relation

$$(1 + \gamma \mathcal{R}) \mathcal{L}_h S = (\gamma - 1)(\mathcal{R} - \mathcal{G}) \frac{\partial S}{\partial t} + B \mathcal{G} \frac{\partial P}{\partial t} + B \frac{\chi}{c^2} \text{div } \mathbf{g} + (1 + \mathcal{R}) \frac{\sigma}{\rho c_p T}. \tag{25}$$

In Eq. (25) the first two terms on the right represent the $O(\tilde{\epsilon}_\kappa)$ residual error that is introduced in the unforced equation by defining $\Phi = S$ (rather than $S - \tilde{\lambda}_a P$), and by approximating the \mathcal{L}_h operator as in Eq. (24). Omission of these terms is therefore justified in the context of the desired $\Delta = O(\tilde{\epsilon})$ approximation. The last two terms represent excitation of the entropy mode by volume sources (σ, \mathbf{g}); they may be represented by $\Delta = O(\tilde{\epsilon})$ approximations, noting that the \mathcal{R} and \mathcal{G} operators are both $O(\tilde{\epsilon})$.

Hence the forced entropy-mode equation can be approximated with relative error $O(\tilde{\epsilon})$ by

$$\mathcal{L}_h S \simeq B \frac{\chi}{c^2} \text{div } \mathbf{g} + \frac{\sigma}{\rho c_p T}. \tag{26}$$

2. Example 2: Acoustic mode equation with $\tilde{\epsilon}_\kappa \ll 1$ and relative error $\Delta = O(\tilde{\epsilon}_\kappa)$

This example describes the derivation of the forced acoustic-mode equation in row 1 of Table I. In this case $\tilde{\epsilon}_L$ is unrestricted and the relative error is $O(\tilde{\epsilon}_\kappa)$. An approximate acoustic variable Ψ can be found by truncating Eq. (A3) at order $i\epsilon_\kappa$, substituting \mathcal{R} and \mathcal{G} for $-i\epsilon_\kappa$ and $-i\epsilon_L$ to give an approximate polarization operator $\tilde{\lambda}_h$, and defining Ψ as

$$\Psi = (1 + \mathcal{R})^2 [(1 + \mathcal{R}) P - A \mathcal{R} S] + (1 + \gamma \mathcal{R}) A \mathcal{G} S. \tag{27}$$

Note that we have multiplied P in the first term by $(1 + \mathcal{R})^3$ to avoid the presence of inverse time-domain operators. The acoustic variable Ψ contains contributions from S that must be retained even though they are of relative order ϵ_κ because taking their Laplacian introduces a large factor $1/\epsilon_\kappa$. It can be verified by direct substitution that omitting these S terms leads to an $O(1)$ residual in $\mathcal{L}_a \Psi$.

At the specified level of approximation Eq. (A6) gives $X_a^{-1} \simeq 1 - i\epsilon_L - [(\gamma - 1)/(1 - i\epsilon_L)] i\epsilon_\kappa$, from which the

corresponding time-domain propagation operator can be found to be

$$\mathcal{L}_a \Psi = \left\{ \frac{\partial^2}{\partial t^2} - \left[(1 + \mathcal{R}) + \frac{(\gamma - 1)\mathcal{G}}{1 + \mathcal{R}} \right] c^2 \nabla^2 \right\} \Psi. \quad (28)$$

The \mathcal{G} term provides long-range attenuation due to heat conduction, but it does not affect the local accuracy of the acoustic mode equation as will be demonstrated below. We shall therefore omit it to begin with, and use the linearized fluid-motion equations to evaluate

$$\mathcal{L}'_a \Psi = \left\{ \frac{\partial^2}{\partial t^2} - (1 + \mathcal{R})c^2 \nabla^2 \right\} \Psi. \quad (29)$$

Equations (22) and (23) can be used to show that

$$c^2 \nabla^2 [(1 + \mathcal{R})P - A\mathcal{R}S] = \text{div } \mathbf{g} - A \frac{\partial^2 S}{\partial t^2} + \frac{\partial^2 P}{\partial t^2}. \quad (30)$$

Combining Eq. (30) with Eq. (27) and then using Eq. (23) gives

$$\begin{aligned} c^2 \nabla^2 \Psi &= (1 + \mathcal{R})^2 \left[\text{div } \mathbf{g} - A \frac{\partial^2 S}{\partial t^2} + \frac{\partial^2 P}{\partial t^2} \right] \\ &\quad + A\mathcal{G}(1 + \gamma\mathcal{R})c^2 \nabla^2 S \\ &= \left[(1 + \mathcal{R})^2 - (\gamma - 1)\mathcal{G} \right] \left(\frac{\partial^2 P}{\partial t^2} + \text{div } \mathbf{g} \right) \\ &\quad - \left[(1 + \mathcal{R})\mathcal{R} - (\gamma - 1)\mathcal{G} \right] A \frac{\partial^2 S}{\partial t^2} \\ &\quad - A(1 + \mathcal{R})\mathcal{G} \frac{c^2 \sigma}{\kappa T}. \end{aligned} \quad (31)$$

Substituting this result in Eq. (29) leads, after some cancellation, to the exact relation

$$\begin{aligned} \mathcal{L}'_a \Psi &= -(1 + \mathcal{R})^3 \text{div } \mathbf{g} + a(1 + \mathcal{R})^2 \frac{\partial \sigma}{\partial t} \\ &\quad + (\gamma - 1)\mathcal{G}(1 + \mathcal{R}) \left(\frac{\partial^2 P}{\partial t^2} + \text{div } \mathbf{g} \right) \\ &\quad + (2 - \gamma + \mathcal{R})A\mathcal{G} \frac{\partial^2 S}{\partial t^2}, \end{aligned} \quad (32)$$

where $a = \alpha/\rho c_p$.

In Eq. (32) the terms in P and S represent the expected $O(\tilde{\epsilon}_\kappa)$ residual error introduced in the unforced equation by defining Ψ as in Eq. (27) and by approximating the \mathcal{L}_a operator as in Eq. (29). Omission of these terms is therefore consistent with the specified $\Delta = O(\tilde{\epsilon}_\kappa)$ approximation.

Likewise the difference between $\mathcal{L}_a \Psi$ and $\mathcal{L}'_a \Psi$, represented by the \mathcal{G} term in Eq. (28), can be obtained from Eq. (31) and consists of similar $O(\tilde{\epsilon}_\kappa)$ terms in P and S that can be neglected, together with $O(\tilde{\epsilon}_\kappa)$ correction terms in \mathbf{g} and σ . Thus, the forced acoustic mode equation for viscous fluids finally becomes

$$\mathcal{L}_a \Psi \simeq -(1 + \mathcal{R})^3 \text{div } \mathbf{g} + (1 + \mathcal{R})^2 a \frac{\partial \sigma}{\partial t} \quad (\tilde{\epsilon}_\kappa \ll 1) \quad (33)$$

with relative error $\Delta = O(\tilde{\epsilon}_\kappa)$. The forcing terms have been approximated in Eq. (33) by omitting contributions of relative order $\tilde{\epsilon}_\kappa$, as in Eq. (26) previously.

3. Summary of time-domain equations for the unbounded case

The time-domain acoustic and entropy mode equations obtained in this way, approximated to different orders in $(\tilde{\epsilon}_\kappa, \tilde{\epsilon}_L)$, are shown in Table I. The terms on the right of Eq. (33) are the forcing terms shown in row 1 of Table I.

The unforced acoustic and entropy mode equations in Table I can all be verified by direct substitution, if one uses the relations above and sets $(\sigma, \mathbf{g}) = 0$; the residual error in each case, expressed as a fraction Δ of either of the terms on the left of the equation, is specified in the first column of the table. The forcing terms in the right-hand column have been obtained by evaluating the left-hand side directly, using the linearized equations for $(\sigma, \mathbf{g}) \neq 0$, and are subsequently approximated to the same relative accuracy.

D. Bounded-region modal equations

Bounded-region formulations can be derived from the corresponding equations in Table I, by introducing a spatial window function $H(f)$ as a multiplying factor in the wave variable and using the Laplacian identity $\nabla^2(H\psi) = (\nabla^2\psi)H + (\hat{\mathbf{n}} \cdot \nabla\psi)\delta(f) + \text{div}[\psi\hat{\mathbf{n}}\delta(f)]$. Here, $H(f)$ is the unit step function, whose derivative is the Dirac delta function $\delta(f)$. The indicator function $f(\mathbf{x})$ is chosen to be positive in the fluid region of interest \mathcal{V} , and negative in the complementary region $\bar{\mathcal{V}}$; thus H equals 1 in \mathcal{V} and 0 in $\bar{\mathcal{V}}$, with $f=0$ on their common interface $\bar{\mathcal{S}}$. By choosing $|\nabla f| = 1$ on $\bar{\mathcal{S}}$ we get $\nabla H = \hat{\mathbf{n}}\delta(f)$, where $\hat{\mathbf{n}}$ is the unit vector normal to $\bar{\mathcal{S}}$ pointing into \mathcal{V} . For this purpose, we note that derivatives of the form $(\partial/\partial x_i)(\psi H)$, where $\psi(\mathbf{x}, t)$ is any continuous function defined for $\mathbf{x} \in \mathcal{V}$, are given by

$$\frac{\partial}{\partial x_i} [\psi(\mathbf{x}, t)H(f)] = \frac{\partial \psi}{\partial x_i} H(f) + \psi \hat{n}_i \delta(f), \quad (34)$$

with ψ and $\partial\psi/\partial x_i$ on the right-hand side interpreted as their values at $f = 0^+$.

The results of this procedure are shown in Table II, where the rows are numbered from zero so that cases occurring in both Table I and Table II have the same row number. As in Table I, the source terms in the right-hand column of Table II are obtained by evaluating the left side of each equation. The forcing terms in (σ, \mathbf{g}) and the boundary terms are both approximated to the stated accuracy in terms of $(\tilde{\epsilon}_L, \tilde{\epsilon}_\kappa)$.

For the normal-gradient boundary terms that arise from windowing, one can either leave these in terms of $\hat{\mathbf{n}} \cdot \nabla P$ and $\hat{\mathbf{n}} \cdot \nabla S$, or else substitute the normal gradients with the aid of Eqs. (35) and (36) below. The second option has been followed in deriving the boundary terms of Table II; its advantage is that $\hat{\mathbf{n}} \cdot \nabla P$ and $\hat{\mathbf{n}} \cdot \nabla S$ are expressed in terms of kinematic quantities plus the normal temperature gradient,

TABLE II. Bounded-region time-domain formulations for linear acoustic and entropy modes in a viscous heat-conducting fluid; for the corresponding vorticity-mode equation, see Sec. V. The boundary surface S is assumed to be fixed but permeable. The validity of retaining the underlined entropy-mode term for $\Delta = O(\tilde{\epsilon})$ depends on individual circumstances; see Sec. III E and Table IV below.

Case	Mode variable	Forced mode equation for bounded region $f > 0$, with fixed boundary $\tilde{S}(f=0)$
0	Arbitrary $(\tilde{\epsilon}_L, \tilde{\epsilon}_\kappa)$; acoustic mode with $\alpha = 0^a$	$\Psi = P = p' / \rho c^2$ $\left\{ \frac{\partial^2}{\partial t^2} - (1 + \mathcal{R})c^2 \nabla^2 \right\} (PH) = \frac{\partial}{\partial t} [u_n \delta(f)] - \text{div} [(\mathbf{g}H) - \nu(\boldsymbol{\omega} \times \hat{\mathbf{n}}) \delta(f)] - \text{div} [(1 + \mathcal{R})c^2 P \hat{\mathbf{n}} \delta(f)]$
1	Arbitrary $\tilde{\epsilon}_L, \tilde{\epsilon}_\kappa \ll 1$; acoustic mode, $\Delta = O(\tilde{\epsilon}_\kappa)^b$	$\Psi = (1 + \mathcal{R})^3 P - A[(1 + \mathcal{R})^2 \mathcal{R} - (1 + \gamma \mathcal{R}) \mathcal{G}] S$ $\left\{ \frac{\partial^2}{\partial t^2} - (1 + \mathcal{R})c^2 \nabla^2 \right\} (\Psi H) \simeq (1 + \mathcal{R})^3 \frac{\partial}{\partial t} [u_n \delta(f)] + (1 + \mathcal{R})^2 \frac{\partial}{\partial t} [\sigma H + q_n \delta(f)] - (1 + \mathcal{R})^3 \text{div} [(\mathbf{g}H) - \nu(\boldsymbol{\omega} \times \hat{\mathbf{n}}) \delta(f)] - \text{div} [(1 + \mathcal{R})c^2 \Psi \hat{\mathbf{n}} \delta(f)]$
2	Arbitrary $\tilde{\epsilon}_L, \tilde{\epsilon}_\kappa \ll 1$; entropy mode, $\Delta = O(\tilde{\epsilon}_\kappa)$	$\Phi = S = s' / c_p$ $\left\{ (1 + \mathcal{R}) \frac{\partial}{\partial t} - (1 + \gamma \mathcal{R}) \chi \nabla^2 \right\} (\Phi H) \simeq \frac{1 + \mathcal{R}}{\rho c_p T} [\sigma H + q_n \delta(f)] - \frac{\alpha \chi}{c_p} \frac{\partial}{\partial t} [u_n \delta(f)] + \frac{\alpha \chi}{c_p} \text{div} [(\mathbf{g}H) - \nu(\boldsymbol{\omega} \times \hat{\mathbf{n}}) \delta(f)] - \text{div} [(1 + \gamma \mathcal{R}) \chi \Phi \hat{\mathbf{n}} \delta(f)]$
3	$(\tilde{\epsilon}_L, \tilde{\epsilon}_\kappa) \ll 1$; acoustic mode, $\Delta = O(\tilde{\epsilon})^b$	$\Psi = P - A(\mathcal{R} - \mathcal{G}) S$ $\left\{ \frac{\partial^2}{\partial t^2} - c^2 \nabla^2 \right\} (\Psi H) \simeq \frac{\partial}{\partial t} [u_n \delta(f)] + a \frac{\partial}{\partial t} [\sigma H + q_n \delta(f)] - \text{div} [(\mathbf{g}H) - \nu(\boldsymbol{\omega} \times \hat{\mathbf{n}}) \delta(f)] - \text{div} [c^2 \Psi \hat{\mathbf{n}} \delta(f)]$
4	$(\tilde{\epsilon}_L, \tilde{\epsilon}_\kappa) \ll 1$; entropy mode, $\Delta = O(\tilde{\epsilon})$	$\Phi = S$ $\left\{ \frac{\partial}{\partial t} - \chi \nabla^2 \right\} (\Phi H) = \frac{1}{\rho c_p T} [\sigma H + q_n \delta(f)] - \frac{\alpha \chi}{c_p} \frac{\partial}{\partial t} [u_n \delta(f)] + \frac{\alpha \chi}{c_p} \text{div} [(\mathbf{g}H) - \nu(\boldsymbol{\omega} \times \hat{\mathbf{n}}) \delta(f)] - \text{div} [\chi \Phi \hat{\mathbf{n}} \delta(f)]$

^aThis exact result for a fluid with zero thermal expansivity is derived in Morfey *et al.* (2012).

^bIn this table, the number of terms retained in the acoustic wave operator is the minimum required for the linear-mode equation to be asymptotically valid locally to the stated accuracy. Compare Table I, notes (b) and (c). Changing the acoustic wave operator to allow for thermoviscous attenuation, as in the corresponding rows of Table I, does not alter the boundary terms or external-source terms to the stated accuracy.

which can be convenient for matching conditions at a solid boundary. The gradient relations required are, from Eqs. (8), (10), and (11),

$$(1 + \gamma \mathcal{R})c^2 \nabla P = \mathbf{g} - \frac{\partial \mathbf{u}}{\partial t} - \frac{\mu}{\rho} \text{curl } \boldsymbol{\omega} + \frac{c^2}{T} A \mathcal{R} \nabla T', \quad (35)$$

$$(1 + \gamma \mathcal{R})c^2 \nabla S = -B \left(\mathbf{g} - \frac{\partial \mathbf{u}}{\partial t} - \frac{\mu}{\rho} \text{curl } \boldsymbol{\omega} \right) + \frac{c^2}{T} (1 + \mathcal{R}) \nabla T'. \quad (36)$$

Note that of the two external inputs (σ, \mathbf{g}), only \mathbf{g} appears in the gradient relations above since they follow directly from the momentum equation, without involving the entropy equation. Equations (35) and (36), like Eqs. (22) and (23) are exact consequences of the linearized equations of fluid dynamics. Together with the appropriate small- $\tilde{\epsilon}_L$ and small- $\tilde{\epsilon}_\kappa$ approximations, they form the basis of Tables I and II.

E. Approximation errors in Tables I and II

In order to describe the time-domain modal variables (Ψ, Φ) we have used small- $\tilde{\epsilon}_\kappa$ or small- $\tilde{\epsilon}$ approximations, which means that the unforced mode equations in Table I fail to balance exactly. The residual error in each case can be obtained from the linearized equations above by direct substitution. The error magnitude Δ , relative to either term in the wave operator, is indicated in the table as either $O(\tilde{\epsilon}_\kappa^n)$ or $O(\tilde{\epsilon}^n)$.

The boundary source terms shown in Table II follow directly from the corresponding $\mathbf{x} \in \mathcal{V}$ mode equation in Table I when the mode variable is replaced with its spatially windowed version. Because of the approximations noted above, in some applications the response to a particular boundary source term may be of higher order in $\tilde{\epsilon}$ (or $\tilde{\epsilon}_\kappa$) than the modal equation concerned is justified in retaining. This will depend on individual circumstances; an example is discussed in Sec. III F (see Table IV). To cover all possibilities, a complete set of boundary terms is provided in Table II, recognizing that in any individual case some of these may not be relevant.

An underlying assumption of the asymptotic analysis leading to all these results is that the dimensionless amplitudes of the acoustic and entropy modes, defined as the maximum amplitudes of the modal variables Ψ and Φ within the fluid region of interest, are both of the same order with respect to $\tilde{\epsilon}$. For further discussion on this point, see Appendix B.

F. Entropy-mode and acoustic-mode source terms compared

Two tables below compare the source terms from Table II that drive the entropy mode with those responsible for generating the acoustic mode. The level of asymptotic approximation chosen is $\Delta = O(\tilde{\epsilon})$. In order to emphasise

TABLE III. Comparison of thermal-type source terms appearing in the acoustic-mode and entropy-mode equations. Results based on the $\Delta = O(\tilde{\varepsilon})$ approximation, corresponding to rows 3 and 4 of Table II.

	Forcing mechanism	Γ_Ψ (acoustic mode)	Γ_Φ (entropy mode)
1	Boundary heat flux	$a \frac{\partial}{\partial t} [q_n \delta(f)]$	$\frac{1}{\rho c_p T} q_n \delta(f)$
2	Distributed heat input	$a \frac{\partial}{\partial t} [\sigma H(f)]$	$\frac{1}{\rho c_p T} \sigma H(f)$

the similarities, the source terms have been grouped into “thermal” and “mechanical” categories, with the former shown in Table III, and the latter in Table IV.

For purposes of Tables III and IV the mode variables are defined as the windowed variables $\Psi H(f)$ and $\Phi H(f)$, with $\Psi = P - A(\mathcal{R} - \mathcal{G})S$ and $\Phi = S$. Consistently with the $\Delta = O(\tilde{\varepsilon})$ local approximation, the corresponding source distributions Γ_Ψ, Γ_Φ are then defined by

$$\left[\frac{\partial^2}{\partial t^2} - c^2 \nabla^2 \right] (\Psi H) = \Gamma_\Psi, \quad \left[\frac{\partial}{\partial t} - \chi \nabla^2 \right] (\Phi H) = \Gamma_\Phi, \quad (37)$$

as in rows 3 and 4 of Table II. Both tables show that the forcing terms for the two modes are closely related; the ratio of Γ_Φ/χ to Γ_Ψ/c^2 is $-B$ for “mechanical” excitation, while for “thermal” excitation with time factor $\exp(-i\omega t)$ it is $i/A\varepsilon_\kappa$. This close connection will allow us in Sec. III G to compare acoustic-mode and entropy-mode responses to specific localized forcing models; the asymptotic validity of the respective response estimates can then be tested against the criteria developed in Appendix B.

As an example of boundary source terms becoming too small to justify retention at the level of approximation adopted, we note that the underlined entropy-mode terms in Table IV describe the scattering of vorticity-mode perturbations incident on a rigid boundary into entropy-mode perturbations. The effect is very weak, however, with the scattered entropy field being of relative order $\tilde{\varepsilon}_\mu^{1/2} \tilde{\varepsilon}_\kappa^{1/2}$ (where $\tilde{\varepsilon}_\mu = \mu/\rho c^2 \tilde{\tau}$), for which the $\Delta = O(\tilde{\varepsilon})$ approximation is insufficient according to the criteria in Appendix B. The underlined Γ_Φ terms would thus not be relevant in that application.

It is important to recall that beside the terms listed in Tables III and IV above, each of the source distributions

$(\Gamma_\Psi, \Gamma_\Phi)$ also contains a normal-dipole boundary term as shown in Table II. If required, one can eliminate the normal-dipole contributions to Ψ or Φ by using the appropriate Neumann Green’s function, G_N , that satisfies the zero normal-gradient condition $\partial G_N/\partial n = 0$ on the boundary.

G. Relative responses of entropy and acoustic modes

In this section we compare the modal responses of an unbounded thermoviscous fluid to various idealized single-frequency sources. The discussion is based on the acoustic mode equation in row 3 of Table I, and the entropy mode equation in row 4. Two main conclusions can be drawn from the results. First, the entropy and acoustic mode responses to the same physical input can differ by an $O(\tilde{\varepsilon}_\kappa)$ factor in the near field, thus locally invalidating the $\Delta = O(\tilde{\varepsilon})$ approximation. Second, the response ratio depends strongly on geometry, with point sources giving different results from plane source layers.

1. Point-source free-field responses

Entropy-mode and acoustic-mode responses are compared for two types of point source, first a single-frequency point force, and then a single-frequency point heat input. The free-field Green’s function for the 3D Helmholtz operator $\nabla^2 + k_{a,h}^2$ is $(1/4\pi r) \exp i k_{a,h} r$. Thus, in the near field with $|k_{a,h}|r \ll 1$, the same Green’s function $(1/4\pi r)$ and Green’s function gradient apply to both the acoustic and entropy modes.

It follows from Table IV that for a point force the respective modal responses (S_h, P_a) in the near field are in the ratio

$$\frac{S_h}{P_a} \simeq \frac{\Phi}{\Psi} = \frac{\Gamma_\Phi/\chi}{\Gamma_\Psi/c^2} = -B. \quad (38)$$

The fact that the responses are the same order in ε means that the $\Delta = O(\varepsilon)$ approximation can legitimately be used, according to the criteria derived in Appendix B.

On the other hand, for single-frequency point sources of heat the corresponding ratio S_h/P_a is $i/A\varepsilon_\kappa$ based on Table III. The near-field response (at radii less than the thermal penetration depth, $l_h = \sqrt{\chi/\omega}$) is dominated in this

TABLE IV. Comparison of mechanical-type source terms appearing in the acoustic-mode and entropy-mode equations. In row 2, $\zeta_n = \hat{\mathbf{n}} \cdot \text{curl } \boldsymbol{\omega}$. Results are based on the $\Delta = O(\tilde{\varepsilon})$ approximation, corresponding to rows 3 and 4 of Table II.

	Forcing mechanism	Γ_Ψ (acoustic mode)	Γ_Φ (entropy mode)
1	Normal boundary velocity	$\frac{\partial}{\partial t} [u_n \delta(f)]$	$-\frac{\alpha \chi}{c_p} \frac{\partial}{\partial t} [u_n \delta(f)]$
2	Tangential boundary vorticity	$\nu \zeta_n \delta(f)$	$-\frac{\alpha \chi}{c_p} \nu \zeta_n \delta(f)$
3	Tangential boundary vorticity (alternative form)	$\text{div} [\nu (\boldsymbol{\omega} \times \hat{\mathbf{n}}) \delta(f)]$	$-\frac{\alpha \chi}{c_p} \text{div} [\nu (\boldsymbol{\omega} \times \hat{\mathbf{n}}) \delta(f)]$
4	Distributed body force	$-\text{div} [\mathbf{g} H(f)]$	$\frac{\alpha \chi}{c_p} \text{div} [\mathbf{g} H(f)]$

case by the entropy mode, as one might expect. Although the $\Delta = O(\varepsilon)$ acoustic-mode solution is still valid at sufficiently large distances from the source (since the entropy mode continues to decay exponentially outside the thermal layer), it may not be used within that layer. The reason is that the amplitude ratio $S_h/P_a \sim O(\varepsilon_\kappa^{-1})$ is too large, according to Appendix B, to justify use of the $\Delta = O(\varepsilon)$ approximation. In order to describe the near acoustic field accurately, one would need to proceed to $\Delta = O(\varepsilon^2)$.

2. Plane source layer responses

A similar comparison is carried out next for three types of plane source layer. The following are considered in turn, each located in the plane $y = 0$: (i) a tangential force distribution in the x direction, (ii) a normal force distribution, and (iii) a heat input distribution. The input quantity in each case is assumed proportional to $e^{i(mx-\omega t)}$. The free-field Green’s function $g_i(y|y_0)$ for either mode is the outgoing-wave solution of

$$\left(\frac{\partial^2}{\partial y^2} + K_i^2\right)g_i(y|y_0) = -\delta(y - y_0) \quad (i = a, h), \quad (39)$$

where $K_i^2 = k_i^2 - m^2$. Hence,

$$g_i(y|y_0) = \frac{i}{2K_i} \exp iK_i|y - y_0|$$

and

$$\frac{\partial g_i}{\partial y_0}(y|y_0) = \frac{1}{2} \operatorname{sgn}(y - y_0) \exp iK_i|y - y_0|. \quad (40)$$

In the limit $|y - y_0| \rightarrow 0$, the following results are obtained for the three cases defined above.

Case (i): This is a mechanical input, of monopole order (no y derivatives). Using Table IV gives the response ratio adjacent to the tangential-force layer as

$$\frac{S_h}{P_a} \simeq \frac{\Phi}{\Psi} = -B \frac{g_h}{g_a} = -B \frac{K_a}{K_h}. \quad (41)$$

If $m/k_0 = O(1)$, where $k_0 = \omega/c_0$ is the lossless acoustic wavenumber, then the ratio $K_a/K_h = O(\varepsilon_\kappa)$. Equation (41) then predicts that the near field is dominated by the acoustic mode. The $O(\varepsilon_\kappa)$ relative smallness of the entropy-mode response means, according to Appendix B, that the $\Delta = O(\varepsilon)$ approximation is inadequate to this situation and if one wished to describe the entropy mode accurately for case (i), one would need to proceed to $\Delta = O(\varepsilon^2)$.

Case (ii): This is also a mechanical input, but of dipole order (single y derivative). Using Table IV gives the response ratio adjacent to the layer as

$$\frac{S_h}{P_a} \simeq \frac{\Phi}{\Psi} = -B \quad \text{since} \quad \frac{\partial g_h/\partial y_0}{\partial g_a/\partial y_0} = 1. \quad (42)$$

Equation (42) predicts that $S_h/P_a = O(1)$; thus, the acoustic and entropy modes are excited with comparable amplitudes.

Case (iii): This is a thermal input, of monopole order (no y derivatives). Using Table III gives the response ratio adjacent to the heat-input layer as

$$\frac{S_h}{P_a} \simeq \frac{\Phi}{\Psi} = \left(\frac{i}{A\varepsilon_\kappa}\right) \frac{g_h}{g_a} = \left(\frac{i}{A\varepsilon_\kappa}\right) \frac{K_a}{K_h}. \quad (43)$$

If $m/k_0 = O(1)$, the ratio $K_a/K_h = O(\varepsilon_\kappa^{1/2})$. Equation (43) then predicts that $S_h/P_a = O(\varepsilon_\kappa^{-1/2})$; the entropy mode is excited much more strongly by a heat-input layer than the acoustic mode. Unlike case (i), however, the disparity is not so great as to invalidate the $\Delta = O(\varepsilon)$ approximation.

A detailed calculation provides the following solution for the total field in the lowest-order approximation [$\Delta = O(\varepsilon)$], due to a normal-force input F_y per unit area and a heat input rate Q per unit area both applied in the plane $y = 0$,

$$S(y = 0^+) \simeq \frac{1}{2} \left(\frac{i}{\varepsilon_\kappa}\right)^{1/2} \frac{Q}{\rho c c_p T} - \frac{1}{2} a F_y, \quad (44)$$

$$P(y = 0^+) \simeq \frac{1}{2} \left(\frac{aQ}{\beta c} + \frac{F_y}{\rho c^2}\right). \quad (45)$$

Here, $\beta = [1 - (m/k_0)^2]^{1/2}$. Equations (44) and (45) give $(S/P)_{y=0^+} = (i/\varepsilon_\kappa)^{1/2} \beta/A$ for Q forcing and $(S/P)_{y=0^+} = -B$ for F_y forcing, in agreement with the general conclusions above.

Tables I and II comprise the main result of this work. They generalize the Kirchhoff–Helmholtz representation, in differential form, to real fluids. In the sections that follow we examine the implications of these equations and explain how they can be used in applications.

IV. EXAMPLE APPLICATION: SOUND RADIATION FROM A PLANE BOUNDARY WITH UNSTEADY HEATING

Consider an infinite plane boundary at $x = 0$ with the halfspace $x > 0$ filled with a uniform fluid initially at rest. The fluid is excited at the boundary by a spatially uniform time-varying heat flux $q_n = \hat{q}_n e^{-i\omega t}$, which drives both the acoustic and entropy modes. The entropy mode response consists of an unsteady thermal boundary layer, whose thickness is of order $l_h = \sqrt{\chi/\omega}$; this is necessarily small compared with the acoustic wavelength in view of our assumption $\varepsilon_\kappa \ll 1$. To estimate the acoustic response, we use the acoustic mode equation in its single-frequency one-dimensional form, based on the $\Delta = O(\varepsilon)$ time-domain version in row 3 of Table II. The governing equation for the acoustic mode variable, valid for all x , is

$$\left\{\frac{d^2}{dx^2} + k_0^2\right\}(\hat{\Psi}H) \simeq i\omega \frac{a}{c^2} \hat{q}_n \delta(x) + \frac{d}{dx} \left[\hat{\Psi} \delta(x)\right] \triangleq -\hat{\Xi}(x). \quad (46)$$

The acoustic-mode eigenvalue k_a^2 is here approximated by $k_0^2 = (\omega/c)^2$ on the basis that thermoviscous attenuation of

sound may be neglected. Equation (46) is to be solved subject to the outgoing-wave condition in $x > 0$, namely, $d(\hat{\Psi}H)/dx = (d/dx)\hat{\Psi}(x) = ik_0\hat{\Psi}$.

Any desired homogeneous boundary condition can be applied in $x < 0$, since $H = 0$ in this region. In order to eliminate the dipole term in Eq. (46) we use a Neumann Green's function $g(x|\xi)$ whose value g^+ in $x > \xi$ represents outgoing waves, and whose gradient $\partial g^+/\partial \xi$ vanishes as $\xi \rightarrow 0$. The Green's function that satisfies these conditions and the equation

$$\left(\frac{d^2}{dx^2} + k_0^2\right)g(x|\xi) = -\delta(x - \xi) \tag{47}$$

is

$$g^+(x|\xi) = \frac{i}{k_0}e^{ik_0x} \cos k_0\xi. \tag{48}$$

The solution of Eq. (46) in $x > 0$ follows as

$$\hat{\Psi}H = \hat{\Psi}(x) = \int_{-\infty}^x \hat{\Xi}(\xi)g^+(x|\xi) d\xi \tag{49}$$

$$= \frac{a}{c}\hat{q}_n e^{ik_0x}. \tag{50}$$

Our use of the Neumann Green's function (48) means that the dipole term $d/dx[\hat{\Psi}\delta(x)]$ on the right of Eq. (46) does not contribute to the solution.

The pressure radiated outside the thermal boundary layer is given by Eq. (50) as

$$\hat{p}(x) \simeq \rho c^2 \hat{\Psi} \simeq \rho c a \hat{q}_n e^{ik_0x}; \tag{51}$$

the relative error in this approximation is $\Delta = O(\varepsilon)$. The simple relation above connects the radiated sound with the boundary heat flux, for any thermoviscous fluid.

The spherical-wave counterpart of Eq. (51) can be obtained similarly. In this case a uniform heat flux $\hat{q}_n e^{-i\omega t}$ is applied over the surface of a rigid sphere of radius r_0 . The corresponding Neumann Green's function is

$$g^+(r|\xi) = \frac{1}{\xi} \left(\frac{r_0}{r}\right) \frac{e^{ik_0(r-r_0)}}{1 - ik_0 r_0} \times \left[\cos k_0(\xi - r_0) + \frac{1}{k_0 r_0} \sin k_0(\xi - r_0) \right] \tag{52}$$

$(r > \xi \geq r_0),$

whose gradient $\partial g^+/\partial \xi$ vanishes as $\xi \rightarrow r_0$. The radiated pressure follows as

$$\hat{p}(r) \simeq \rho c^2 \hat{\Psi}, \quad \hat{\Psi}(r) = \left(\frac{r_0}{r}\right) \frac{a \hat{q}_n}{c} \frac{e^{ik_0(r-r_0)}}{1 + i/k_0 r_0}. \tag{53}$$

If, however, the fluid is excited by a specified boundary temperature fluctuation $T' = \hat{\theta} e^{-i\omega t}$ at $x=0$, rather than a specified heat flux, then a relation between $\hat{\theta}$ and \hat{q}_n is needed

in order to apply Eq. (51). This can be supplied by solving the entropy mode equation from row 4 of Table II, whose frequency domain version for the plane-boundary problem is

$$\left\{ \frac{d^2}{dx^2} + k_h^2 \right\} (\hat{\Phi}H) \simeq -\frac{1}{\kappa T} \hat{q}_n \delta(x) + \frac{d}{dx} [\hat{\Phi} \delta(x)] \stackrel{\Delta}{=} -\Upsilon(x). \tag{54}$$

The only change required to the Green's function is to replace k_0 in Eq. (48) by k_h . Once $\hat{\Psi}$ and $\hat{\Phi}$ are known the temperature follows from $T'/T_0 = BP + S$, with $P \simeq \Psi$ and $S \simeq \Phi$. Alternatively, the desired relation can be found using the matching procedure outlined in Sec. VI, where the plane wave solution for a prescribed temperature is obtained in Sec. VIC.

V. VORTICITY MODE IN BOUNDED FLUIDS

Taking the curl of the linearized momentum Eq. (8) and introducing the kinematic viscosity $\nu = \mu/\rho$ leads to a linearized vorticity equation valid in region \mathcal{V} ($f > 0$),

$$\frac{\partial \omega}{\partial t} = \text{curl } \mathbf{g} - \nu \text{curl } \zeta \quad (\zeta = \text{curl } \omega). \tag{55}$$

Equation (55) is the forced vorticity-mode equation that describes the excitation and diffusion of vorticity perturbations in a uniform viscous fluid at rest. A windowed version of this equation, with $\omega H(f)$ in place of ω , can be obtained by multiplying Eq. (55) by $H(f)$ and rearranging. With the aid of various vector calculus relations one obtains the bounded-region vorticity equation

$$\left\{ \frac{\partial}{\partial t} - \nu \nabla^2 \right\} (\omega H) = \text{curl } \mathbf{g} H + (\mathbf{g} - \nu \zeta) \times \hat{\mathbf{n}} \delta(f) - \nu \nabla (\omega_n \delta(f)) - \nu \text{curl} (\omega \times \hat{\mathbf{n}} \delta(f)), \tag{56}$$

where $\omega_n = \omega \cdot \hat{\mathbf{n}}$ is the vorticity component normal to the boundary \mathcal{S} of the excluded region.

The first, third and fourth source terms on the right of Eq. (56) involve spatial derivatives of generalized functions. It is convenient for solution purposes to transfer these derivatives to the vorticity-mode Green's function $G_w(\mathbf{x}, t|\mathbf{y}, \tau)$. The solution for $\omega(\mathbf{x}, t)$ in region \mathcal{V} then takes the form

$$\omega = \int d\tau \left\{ \int_{\mathcal{V}} \frac{1}{\nu} (\mathbf{g} \times \nabla_y G_w) d^3 \mathbf{y} + \int_{\mathcal{S}} \frac{1}{\nu} (\mathbf{g} \times \hat{\mathbf{n}}) G_w dS(\mathbf{y}) + \mathbf{A} \right\}. \tag{57}$$

where the contribution due to boundary vorticity is given by

$$\mathbf{A} = \int_{\mathcal{S}} [\omega_n \nabla_y G_w - (\omega \times \hat{\mathbf{n}}) \times \nabla_y G_w - (\zeta \times \hat{\mathbf{n}}) G_w] dS(\mathbf{y}). \tag{58}$$

Here, $G_w(\mathbf{x}, t|\mathbf{y}, \tau)$ is a solution of the inhomogeneous diffusion equation $(\nu^{-1} \partial/\partial t - \nabla_x^2) G_w = \delta(\mathbf{x} - \mathbf{y}) \delta(t - \tau)$. If the

boundary is a solid wall, substituting the value of $\zeta \times \hat{\mathbf{n}}$ at the wall from Eq. (8) shows how vorticity generation at a no-slip boundary is related to the tangential pressure gradient [Lighthill (1978), p. 131], thus providing a coupling mechanism between the vorticity and acoustic modes. Note that G_w is not uniquely defined; it may be taken as any causal solution valid in $\mathcal{V}_+ \supset \mathcal{V}$. An analogous integral formula for electromagnetic fields is given by Jones (1986).

This formal solution of the linearized vorticity equation shows how the unsteady vorticity in a given domain \mathcal{V} can be related entirely to the vorticity on the domain boundary and to the body force field \mathbf{g} in \mathcal{V} , with no input from the other quantities (σ, u_n, q_n) that drive the acoustic and entropy modes. An analogous conclusion applies to shear waves in a uniform elastic solid, as discussed in Achenbach (1975).

VI. MODAL FIELDS IN TERMS OF POTENTIALS

A. Fundamental relations for thermoviscous fluids

Instead of using Ψ , Φ and the vorticity ω as modal variables as done previously, one can describe the three linear perturbation modes in a source-free fluid region in terms of a triple decomposition of the velocity field using two scalar potentials and a vector potential, $(\varphi_a, \varphi_h, \mathbf{w})$. The modal velocity perturbations then follow as

$$\mathbf{u}_a = \nabla \varphi_a, \quad \mathbf{u}_h = \nabla \varphi_h, \quad \mathbf{u}_w = \text{curl } \mathbf{w}, \quad (59)$$

with $\mathbf{u}_a + \mathbf{u}_h + \mathbf{u}_w = \mathbf{u}$. Our aim in what follows is to relate the modal components of (p', s', T') , represented below in dimensionless form as $P = p'/\rho c^2$, $S = s'/c_p$ and T'/T , to the potentials φ_a and φ_h , and also in reverse to express φ_a and φ_h in terms of P_a and S_h . It will be assumed that no volume sources are present. Then away from boundaries the three modes propagate independently with no first-order coupling, and the linearized continuity equation can be split into separate acoustic and entropy mode components to give

$$\nabla^2 \varphi_i = -\frac{\partial P_i}{\partial t} + A \frac{\partial S_i}{\partial t} \quad (i = a, h). \quad (60)$$

It is convenient to assume all quantities are proportional to $e^{-i\omega t}$. Since there are no external sources, φ_a and φ_h obey the homogeneous equations

$$\nabla^2 \varphi_i = -k_i^2 \varphi_i \quad (i = a, h). \quad (61)$$

with k_a^2 and k_h^2 given by the dispersion relations in Appendix A. Also, P_i and S_i for each mode are connected by the frequency-domain polarization relations

$$S_a = \lambda_a P_a, \quad P_h = \lambda_h S_h, \quad (62)$$

where the coefficients λ_a, λ_h are given in Appendix A as series expansions in $(-i\varepsilon_L, -i\varepsilon_L)$. It follows from Eqs. (60)–(62) that

$$-i\omega P_a = \frac{k_a^2 \varphi_a}{1 - A\lambda_a} \quad \text{and} \quad -i\omega S_h = \frac{k_h^2 \varphi_h}{\lambda_h - A}. \quad (63)$$

Equations (63) relate P_a and S_h to the scalar potentials φ_a and φ_h in a source-free region. Corresponding relations for P_h and S_a can then be obtained from Eq. (62). The temperature perturbation in either mode follows from the linearized thermodynamic relations

$$\frac{T'_a}{T} = B P_a + S_a, \quad \frac{T'_h}{T} = B P_h + S_h. \quad (64)$$

B. Explicit results for P , S , and T'/T

Equations (60)–(64) are all exact consequences of the linearized equations of fluid motion in a source-free region. Substituting asymptotic expressions for k_a^2, k_h^2, λ_a , and λ_h from Appendix A gives, for thermoviscous fluids,

$$\frac{P_a}{\varphi_a} = \frac{i\omega}{c^2} [1 + i\varepsilon_L - \varepsilon_L^2 - (\gamma - 1)\varepsilon_L \varepsilon_\kappa + O(\varepsilon^3)], \quad (65)$$

$$\frac{S_a}{\varphi_a} = \frac{\omega}{c^2} B \varepsilon_\kappa [1 + 2i\varepsilon_L + (\gamma - 2)i\varepsilon_\kappa + O(\varepsilon^2)], \quad (66)$$

$$\frac{P_h}{\varphi_h} = \frac{-i}{\chi} (\varepsilon_L - \varepsilon_\kappa) [1 + (\gamma - 1)i\varepsilon_L + O(\varepsilon^2)], \quad (67)$$

$$\begin{aligned} \frac{S_h}{\varphi_h} = \frac{1}{\chi A} \{ & 1 + (\gamma - 2)i(\varepsilon_L - \varepsilon_\kappa) - (\gamma - 1) \\ & \times [(\gamma - 1)\varepsilon_L^2 - (\gamma + 1)\varepsilon_L \varepsilon_\kappa + \varepsilon_\kappa^2] + O(\varepsilon^3) \}. \end{aligned} \quad (68)$$

The temperature perturbation then follows from Eq. (64),

$$\begin{aligned} \frac{T'_a/T_0}{\varphi_a} = \frac{i\omega}{c^2} B [& 1 + i(\varepsilon_L - \varepsilon_\kappa) - \varepsilon_L^2 - (\gamma + 1)\varepsilon_L \varepsilon_\kappa \\ & + (\gamma - 2)\varepsilon_\kappa^2 + O(\varepsilon^3)], \end{aligned} \quad (69)$$

$$\frac{T'_h/T_0}{\varphi_h} = \frac{1}{\chi A} [1 - i(\varepsilon_L - \varepsilon_\kappa) + (\gamma - 1)\varepsilon_\kappa(2\varepsilon_L - \varepsilon_\kappa) + O(\varepsilon^3)]. \quad (70)$$

In Eqs. (65)–(70), each modal component of P , S , and T'/T has been expanded up to $O(\varepsilon^2)$. In order to obtain time-domain versions one would substitute the time-domain operators \mathcal{R} and \mathcal{G} for $-i\varepsilon_L, -i\varepsilon_\kappa$ respectively, and replace $-i\omega$ with $\partial/\partial t$.

Various alternative relations, similar to Eqs. (65)–(70), can be found that connect pairs of the acoustic-mode variables $(\varphi_a, P_a, S_a, T'_a)$ in a source-free region; the same applies to the entropy-mode variables $(\varphi_h, P_h, S_h, T'_h)$. Although we have chosen to present our results as series expansions in $(-i\varepsilon_L, -i\varepsilon_L)$, exact versions of all such relations are available in terms of the appropriate inverse eigenvalue $(X_a$ or $X_h)$ (see Appendix C). However, the danger in using these is that if the squared wavenumbers are approximated to a

given order in $(\varepsilon_L, \varepsilon_\kappa)$, the resulting relations are not guaranteed to be accurate to the same order.

C. Example: Relation between temperature and heat flux at a plane boundary

As an illustration of the use of potentials, we continue the half-space problem introduced in Sec. IV by solving for the sound field radiated by a prescribed temperature fluctuation $T' = \hat{\theta}e^{-i\omega t}$ on the boundary. The acoustic and entropy modal potentials for single-frequency excitation are introduced as

$$\varphi_a = \hat{\varphi}_a e^{-i\omega t}, \quad \varphi_h = \hat{\varphi}_h e^{-i\omega t}. \tag{71}$$

Equations (69) and (70) of Sec. VI give the corresponding temperature perturbations as

$$\frac{\hat{T}_a}{T_0} = \frac{i\omega}{c^2} B \varphi_a [1 + O(\varepsilon)], \quad \frac{\hat{T}_h}{T_0} = \frac{1}{\chi A} \varphi_h [1 + O(\varepsilon)]. \tag{72}$$

The boundary conditions to be applied at $x = 0$ are

$$k_a \hat{\varphi}_a + k_h \hat{\varphi}_h = 0, \quad \hat{T}_a + \hat{T}_h = \hat{\theta}; \tag{73}$$

the first condition ensures that the fluid velocity is zero on the boundary. Combining Eqs. (72) and (73) allows one to solve for (\hat{T}_a, \hat{T}_h) in terms of the boundary temperature $\hat{\theta}$, and hence to find the modal components (\hat{q}_a, \hat{q}_h) of the boundary heat flux \hat{q}_n :

$$\hat{q}_a \simeq \varepsilon_\kappa^{1/2} (\gamma - 1) \frac{\kappa \omega}{c} \hat{\theta} e^{i\pi/4}, \quad \hat{q}_h \simeq \varepsilon_\kappa^{-1/2} \frac{\kappa \omega}{c} \hat{\theta} e^{-i\pi/4}. \tag{74}$$

In each case the relative error is $\Delta = O(\varepsilon_\kappa^{1/2}) + O(\varepsilon_L)$. Equation (74) shows that $|\hat{q}_a/\hat{q}_h| = O(\varepsilon_\kappa)$, so the heat flux due to the acoustic mode may be neglected without loss of accuracy.

The radiated pressure field then follows from Eq. (51) as

$$\hat{p}(x) \simeq \varepsilon_\kappa^{-1/2} \frac{\alpha \omega \kappa}{c_p} \hat{\theta} e^{i(k_0 x - \pi/4)} = \varepsilon_\kappa^{1/2} \rho c^2 \alpha \hat{\theta} e^{i(k_0 x - \pi/4)} \tag{75}$$

with the same relative error as in Eq. (74). In order to allow for thermoviscous attenuation, k_0 may be replaced by $k_a \simeq k_0 [1 + \frac{1}{2} i \varepsilon_L + \frac{1}{2} i (\gamma - 1) \varepsilon_\kappa]$ in the exponent of Eq. (75). Equation (75) applies to any thermoviscous fluid, so represents a generalization of the initial analysis of this problem due to Trilling (1955), where the fluid was assumed to be an ideal gas with zero bulk viscosity and shear Prandtl number $\nu/\chi = \frac{3}{4}$.

Comparison of Eq. (75) with the corresponding result Eq. (24) in Trilling (1955), noting that for an ideal gas $\alpha = 1/T$ and $\gamma p = \rho c^2$, shows perfect agreement within the present small- ε approximation.

These results were validated by comparing the predicted pressure at the wall with simulations made using COMSOL MULTIPHYSICS version 6.1 to solve a set of equations

equivalent to Eqs. (7)–(9), but with temperature replacing entropy as a dependent variable.

Although the preliminary analysis in Trilling (1955) is exact, his Eq. (24), which corresponds to our Eq. (75), is in fact a low-frequency approximation. The exact dimensionless wall pressure can be found from the exact eigenvalue $X_a^{-1} = (1 - \gamma i \varepsilon_\kappa)$ for the $Y = 1$ case to be

$$\hat{P}(0) = \hat{P}_a(0) = \alpha \varepsilon_\kappa^{1/2} \hat{\theta} \frac{1 + i \varepsilon_\kappa X_a}{(i X_a)^{1/2} + (\gamma - 1) \varepsilon_\kappa^{1/2}}. \tag{76}$$

The modulus of this expression, normalized by $\alpha \varepsilon_\kappa^{1/2} \hat{\theta}$, is compared with numerical predictions in Fig. 1(a) as a function of ε_κ . The fluid properties used in the numerical simulation were those of air at room temperature but with $\mu_B = 0$ Pa s and κ chosen to give $Y = 1$ as assumed by Trilling (1955). The corresponding frequency range runs from about 1 kHz to 1 GHz although, as noted above, as ε_κ approaches unity continuum theory will break down for gases.

When $Y \neq 1$ both the acoustic and entropy modes will contribute to the pressure field. Their pressure components can be found by matching boundary conditions using potentials and using the relations given in Appendix C and Table VI, with the exact eigenvalues given in Eq. (17). The acoustic-mode wall pressure is

$$\hat{P}_a(0) = \frac{\alpha \hat{\theta}}{Z_a} (1 + i \varepsilon_L X_a) \simeq i^{-1/2} \varepsilon_\kappa^{1/2} \alpha \hat{\theta} [1 + O(\varepsilon_\kappa^{1/2})], \tag{77}$$

where

$$Z_a = \gamma [1 - (X_a/X_h)^{1/2}] - (1 - \gamma i \varepsilon_L) X_a [1 - (X_h/X_a)^{1/2}] \sim \varepsilon_\kappa^{-1/2}. \tag{78}$$

The entropy-mode contribution is given by interchanging the a and h subscripts throughout.

Figure 1(b) shows these expressions, and their $O(\varepsilon_\kappa^1)$ asymptotes, normalized as before by $\alpha \varepsilon_\kappa^{1/2} \hat{\theta}$, and compares the total pressure amplitude with numerical simulations. The same fluid properties were used except that μ was chosen to give a shear Prandtl number of 1 and μ_B was set equal to μ , giving $Y = 7/3$. Although unrealistic for air this allows the contribution of the entropy-mode pressure at high frequencies to be clearly seen.

D. Advantages and limitations of the potential representation

The relations given in Secs. VIB, VIC demonstrate that any of the scalar variables $(\varphi_a, p'_a, s'_a, T'_a)$ can in principle be used to characterize the acoustic mode in a source-free region; the velocity potential φ_a is one option, but for example Cutanda-Henrriquez and Juhl (2013) use p'_a , while Bruneau et al. (1989) and Beltman (1999) use T'_a . Likewise, in the absence of sources the entropy mode can be represented by any one of $(\varphi_h, p'_h, s'_h, T'_h)$; the choice is not constrained by what is used for the acoustic mode, although the

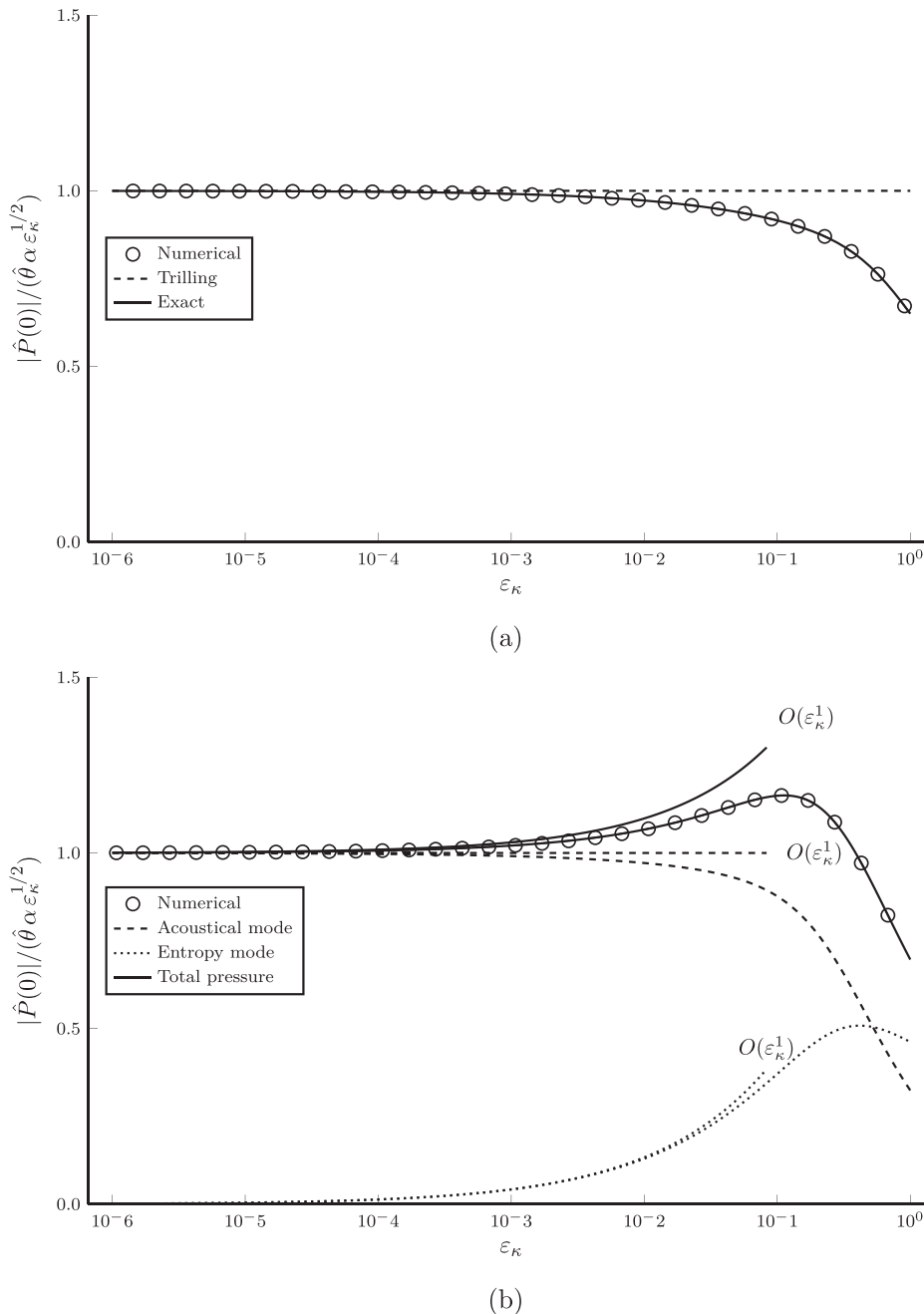


FIG. 1. Comparison of numerical and theoretical predictions of pressure-fluctuation amplitude at a wall whose temperature varies harmonically with time. The fluid simulated is air at 1 bar and 20°C with $c = 343 \text{ ms}^{-1}$, $\nu = 1.6 \times 10^{-5} \text{ m}^2 \text{ s}^{-1}$, $c_p = 1005.7 \text{ J kg K}^{-1}$ and $\gamma = 1.4$. In (a) κ is chosen to make the shear Prandtl number $\text{Pr} = 3/4$ and $\mu_B = 0 \text{ Pa s}$, so that the longitudinal Prandtl number $Y = 1$. In (b) $\text{Pr} = 1$ and $\mu_B = \mu$ so that the longitudinal Prandtl number $Y = 7/3$.

authors cited above use p'_h and T'_h , respectively. The choice of p'_h as entropy mode variable is not recommended because, as Appendix C explains, the entropy mode component of p' vanishes when $Y = 1$. For air at 20°C the value of Y would be 0.96 if the bulk viscosity were zero. However, according to Greenspan (1959) $\mu_B/\mu = 0.6$ due to rotational relaxation, giving $Y = 1.39$.

The distinctive feature of Ψ and Φ as mode variables is that when external volume sources (σ, \mathbf{g}) are present, (Ψ, Φ) obey the inhomogeneous mode equations shown in Tables I and II. The existence in a heat-conducting fluid of two scalar modes, both of which are excited by the same source distributions $(\sigma, \text{div } \mathbf{g})$, means that one cannot formulate separate inhomogeneous equations for

the modal velocity potentials associated with the acoustic and entropy modes. On the other hand, once a solution for the scalar variables (P, S) has been found using Ψ and Φ , the results given above allow one to estimate the potentials φ_a and φ_h outside the source region, and the corresponding modal velocities $(\mathbf{u}_a, \mathbf{u}_h)$ follow by taking their gradients. The rotational velocity field can also be found outside the region where $\text{curl } \mathbf{g} \neq 0$, by using

$$\mathbf{u}_w = k_w^{-2} \text{curl } \boldsymbol{\omega} \quad (k_w^2 = i\omega/\nu), \tag{79}$$

once the inhomogeneous vorticity mode equation in Sec. V has been solved for $\boldsymbol{\omega}$.

**VII. APPLICATION: ACOUSTIC MODE
EXTRAPOLATION FROM MULTIMODE BOUNDARY
DATA**

In this section we consider the excitation of modal fields at boundaries, and assume volume forcing terms are absent. We address the question of whether, in the presence of non-radiating entropy and vorticity fluctuations, data on the fluid normal velocity, normal heat flux, and tangential vorticity at a boundary can provide robust estimates of the radiated acoustic field, in a manner analogous to the ideal-fluid Kirchhoff–Helmholtz formulation based on u_n and p' data.

A. Extrapolation of the acoustic mode from surface data

In thermoviscous fluids, linear extrapolation of the acoustic mode from surface data is complicated by the possible presence of entropy and vorticity modes. Of the three fluid-dynamic quantities u_n , q_n , and $(\boldsymbol{\omega} \times \hat{\mathbf{n}})$ whose values on the boundary surface determine the acoustic field in the generalized Kirchhoff–Helmholtz representation of Sec. III, $(\boldsymbol{\omega} \times \hat{\mathbf{n}})$ is driven by the vorticity mode, q_n will generally contain an entropy mode component as well as an acoustic mode, and u_n may contain contributions from all three. The presence of these modes, for example at a vibrating solid boundary or a boundary with unsteady heating, invalidates the use of the lossless Kirchhoff–Helmholtz integral representation based on u_n and p' at that surface to predict the radiated sound—as has previously been recognized in the textbook by Pierce (1994). The question we wish to address is: How sensitive is the extrapolated field to cross-modal contamination from other modes present in the data, when one uses the generalized theory of Sec. III to predict the sound radiation?

B. Cylindrical-geometry test cases based on analytical modal solutions

As a test of how sensitive the extrapolated sound field is to cross-modal contamination, we consider two cases where all three modes are present on a cylindrical surface $r = r_0$. The first case (a) is an exterior problem: boundary conditions at $r = r_0$ are assumed to drive outgoing waves in all three modes in the region $r > r_0$. In case (b) boundary conditions at $r = r_0$ drive standing waves in the interior space $r < r_0$. The theory of Sec. III is combined with data on u_n , q_n , and $(\boldsymbol{\omega} \times \hat{\mathbf{n}})$ at $r = r_0$ to project the acoustic-mode component into the exterior and interior spaces respectively. The results reveal what contribution the separate modal components of u_n , q_n , and $(\boldsymbol{\omega} \times \hat{\mathbf{n}})$ as boundary conditions would each make to the projected sound field. Although the net contribution of either the vorticity or the entropy mode components is zero, the failure of individual terms to cancel if the surface data are inaccurate represents a potential source of error.

The separable property of the Helmholtz equation in (x, r, θ) cylindrical coordinates means that in the frequency domain one can construct axisymmetric solutions of the

modal equations (i.e., with $u_\theta = 0$ and $\partial\psi/\partial\theta = 0$, where ψ is any scalar property) in the form

$$P_a = C_a R_a(r) e^{i(mx - \omega t)}, \quad S_h = C_h R_h(r) e^{i(mx - \omega t)},$$

$$\left(\frac{ik_w}{c}\right) w_\theta = C_w R_w(r) e^{i(mx - \omega t)}. \tag{80}$$

Here, m is real, and $R_i(r)$ are the radial functions for each mode ($i = a, h, w$), normalized to 1 at $r = r_0$. The radial functions for outgoing waves [case (a)] are

$$R_a(r) = \frac{H_0^{(1)}(K_a r)}{H_0^{(1)}(K_a r_0)}, \quad R_h(r) = \frac{H_0^{(1)}(K_h r)}{H_0^{(1)}(K_h r_0)},$$

$$R_w(r) = \frac{H_1^{(1)}(K_w r)}{H_1^{(1)}(K_w r_0)}, \tag{81}$$

with radial wavenumbers for each mode ($i = a, h, w$) given by $K_i = \sqrt{k_i^2 - m^2}$; while for case (b), $(H_0^{(1)}, H_1^{(1)})$ are replaced by (J_0, J_1) . The vorticity mode ($i = w$) in Eqs. (80) and (81) is characterized by a solenoidal vector potential $\mathbf{w} = (0, 0, w_\theta)$ that obeys $(\nabla^2 + k_w^2)\mathbf{w} = 0$; the vorticity vector then follows from $\boldsymbol{\omega} = -\nabla^2 \mathbf{w} = k_w^2 \mathbf{w}$. The reason that $H_1^{(1)}$ appears in Eq. (81) for $R_w(r)$ is that $[\nabla^2 \mathbf{w}]_\theta \neq \nabla^2 w_\theta$; $[\nabla^2 \mathbf{w}]_\theta$ contains an extra term $-w_\theta/r^2$, which changes the Bessel equation from order 0 (the value for an axisymmetric scalar variable) to order 1.

To relate u_n , q_n , and $(\boldsymbol{\omega} \times \hat{\mathbf{n}})$ on $r = r_0$ to the modal coefficients C_i , we note that for the vorticity mode, $(\boldsymbol{\omega} \times \hat{\mathbf{n}})$ and the normal velocity u_{wn} on $r = r_0$ can be expressed in terms of w_θ by using

$$(\boldsymbol{\omega} \times \hat{\mathbf{n}}) = (\omega_\theta, 0, 0), \quad \omega_\theta = k_w^2 w_\theta,$$

and

$$\mathbf{u}_w = \left(\frac{1}{r} \frac{\partial}{\partial r}(r w_\theta), -\frac{\partial w_\theta}{\partial x}, 0\right). \tag{82}$$

For the acoustic and entropy modes, the normal velocities u_{an} , u_{hn} follow from the respective scalar potentials. The latter can be related to P_a , S_h with relative error $\Delta = O(\varepsilon)$ by inverting Eqs. (65) and (68) to give

$$\varphi_a \simeq \frac{c^2}{i\omega} (1 - i\varepsilon_L) P_a,$$

$$\varphi_h \simeq \chi \alpha T [1 - (2 - \gamma)i(\varepsilon_\kappa - \varepsilon_L)] S_h; \tag{83}$$

taking the radial derivative yields the normal velocities u_{an} , u_{hn} on the cylindrical surface. For case (a), Eq. (81) gives the required radial-function derivatives at $r = r_0$ as

$$R_i'(r_0) = K_i/E_0(z_i),$$

$$E_0(z_i) = H_0^{(1)}(z_i)/H_0^{(1)'}(z_i) \quad (i = a, h), \tag{84}$$

where $z_i = K_i r_0$ is the dimensionless radial wavenumber for each mode. A similar result applies to case (b) with $E_0(z_i)$

replaced by $F_0(z_i) = J_0(z_i)/J'_0(z_i)$. The functions $E_0(z_a)$, $F_0(z_a)$ are closely related to the Neumann acoustic Green's functions for the exterior and interior regions.

Finally, the normal heat flux for each mode is given to the same accuracy by substituting the relations

$$\begin{aligned} \frac{T'_a}{T_0} &\simeq B(1 - i\varepsilon_\kappa)P_a, \\ \frac{T'_h}{T_0} &\simeq [1 - i(\gamma - 1)(\varepsilon_L - \varepsilon_\kappa)]S_h \quad (B = \alpha c^2/c_p) \end{aligned} \quad (85)$$

in $\mathbf{q} = -\kappa\nabla T$, and using Eq. (84) above to obtain the radial derivatives. Equation (85) is based on the linearized thermodynamic relation (64) together with the polarization relations (A4) and (A5).

The non-dimensional modal variables (P_a , S_h) used to characterize the acoustic and entropy modes in Eq. (80) are those used in Sec. III B. One can interpret the acoustic mode amplitude $|C_a|$ either as the amplitude of $p'_a/\rho c^2$ at $r = r_0$, or alternatively (provided $|K_a|r_0 \gg 1$) as the amplitude of $|\mathbf{u}_a|/c$.² For the vorticity mode, the choice of $(ik_w/c)w_\theta$ as variable means that $|C_w| \simeq |\mathbf{u}_w|/c$ in both cases (a) and (b), provided the cylinder radius is much larger than the vorticity-mode length scale $l_w = \sqrt{\nu/\omega}$, so that $|k_w|r_0 \gg 1$, and $m/k_0 = O(1)$. Our initial assumption will be that all three modes are present at $r = r_0$ with similar amplitudes $|C_i|$.

C. Acoustic-mode source terms on $r = r_0$

The governing inhomogeneous equation for boundary-driven axisymmetric acoustic waves in either the exterior region $r > r_0$ or the interior region $r < r_0$ has the general form

$$\begin{aligned} &\left\{ \frac{1}{r} \frac{\partial}{\partial r} \left(r \frac{\partial}{\partial r} \right) + K_a^2 \right\} (P_a H) \\ &= -Q_a \delta(r - r_0) \pm \frac{\partial}{\partial r} [P_a \delta(r - r_0)] \quad (r \gtrless r_0), \end{aligned} \quad (86)$$

where the unit step function $H = H(r - r_0)$ for case (a), $r > r_0$, and $H = H(r_0 - r)$ for case (b), $r < r_0$. For purposes of the present $\Delta = O(\varepsilon)$ analysis the dimensionless acoustic-mode pressure P_a is approximated by the frequency-domain version of Ψ in row 3 of Table II, namely, $P + i(\varepsilon_L - \varepsilon_\kappa)AS$. The surface monopole distribution Q_a for radiation into the exterior space then follows from row 3 of Table II, which when combined with Eq. (82) gives

$$Q_a = -\frac{i\omega}{c^2}(u_r + aq_r) + \frac{\omega m}{c^2}w_\theta. \quad (87)$$

For radiation into the interior region $r < r_0$, the direction of $\hat{\mathbf{n}}$ is reversed and Q_a is the negative of the expression in Eq. (87). Then, if $g(r|\xi)$ is a Green's function for the operator in Eq. (86), defined for either case (a) with $(r, \xi) \geq r_0$ or case (b) with $(r, \xi) \leq r_0$ by

$$\left[\frac{1}{r} \frac{\partial}{\partial r} \left(r \frac{\partial}{\partial r} \right) + K_a^2 \right] g(r|\xi) = -\frac{1}{r} \delta(r - \xi), \quad (88)$$

the acoustic field \tilde{P}_a reconstructed from data on $r = r_0$ is

$$\tilde{P}_a(r) = Q_a(r_0)r_0 g(r|r_0) \pm P_a(r_0)r_0 \frac{\partial g(r|\xi)}{\partial \xi} \Big|_{\xi=r_0}. \quad (89)$$

The + sign in Eq. (89) applies to case (a), and the - sign to case (b).

To solve Eq. (86) for the acoustic field in the exterior region $r > r_0$ using data for Q_a alone, we require the Neumann Green's function $g_N(r|\xi)$ whose normal gradient $\partial g_N/\partial \xi$ vanishes just inside the cylindrical surface at $\xi = r_0 - \epsilon$, in the limit $\epsilon \rightarrow 0$; thus

$$g_N(r|r_0) = -\frac{1}{K_a r_0} \frac{H_0^{(1)}(K_a r)}{H_0^{(1)'}(K_a r_0)}, \quad (90)$$

and for the interior region $r < r_0$, the corresponding Green's function whose normal gradient vanishes just outside the cylindrical surface at $\xi = r_0 + \epsilon$ is

$$g_N(r|r_0) = \frac{1}{K_a r_0} \frac{J_0(K_a r)}{J_0'(K_a r_0)}. \quad (91)$$

The acoustic field projected from data on $r = r_0$ follows from Eq. (89) as $\tilde{P}_a(r) = Q_a(r_0)r_0 g_N(r|r_0)$.

For extrapolation into the interior space $r < r_0$, a disadvantage is the occurrence of resonances, whose effect is to amplify cross-modal contamination associated with errors in the surface data; the effect is quantified in Sec. VII D. Thus in Eq. (91) $J_0'(K_a r_0)$ becomes small and $\tilde{P}_a(r)/Q_a(r_0)$ becomes large, when $k_0^2 - m^2 = (j'_{0q}/r_0)^2$ where j'_{0q} are the stationary values of the J_0 Bessel function. The amplitude at resonance is limited only by fluid-acoustic damping in the interior space.

D. Modal contributions to \tilde{P}_a

Table V shows a breakdown of the modal contributions to the reconstructed exterior field $\tilde{P}_a(r > r_0)$, based on the Neumann Green's function and with the contribution of each monopole source term in Q_a split into modal components.

Thus

$$\begin{aligned} \tilde{P}_a(r > r_0) &= \tilde{C}_a e^{i(mx - \omega t)} R_a(r), \\ \tilde{C}_a &= \Lambda_{aa} C_a + \Lambda_{ah} C_h + \Lambda_{aw} C_w. \end{aligned} \quad (92)$$

The modal coefficients Λ_{ai} that determine the contribution made by each of the three modes ($i = a, h, w$) to the projected sound field are given by adding the separate source-term contributions associated with u_r , q_r , and w_θ , as listed in the column for each coefficient. The Λ_{ah} and Λ_{aw} columns, with $z_a = K_a r_0$ and $z_h = K_h r_0$ as dimensionless parameters, contain terms that in theory should cancel, leaving no net

TABLE V. Coefficients Λ_{ai} in Eq. (92) that determine the outgoing-wave acoustic field in the exterior region $r > r_0$, when u_r , q_r , and w_θ (or $\omega_\theta = k_w^2 w_\theta$) on the cylindrical surface $r=r_0$ are used as data. In the Λ_{ah} column, the correction factors Σ_u , Σ_q are $\Sigma_u = [1 + (2 - \gamma)i(\varepsilon_L - \varepsilon_\kappa)]$, $\Sigma_q = [1 + (\gamma - 1)i(\varepsilon_L - \varepsilon_\kappa)]$. In both the Λ_{aa} and Λ_{ah} columns, each entry is given to $O(\varepsilon)$ relative accuracy. All variables (u_r , q_r , and w_θ) are assumed proportional to $e^{i(m\varphi - \omega t)}$ with m real.

	Input variable	Λ_{aa}	Λ_{ah}	Λ_{aw}
1	u_r	$1 - i\varepsilon_L$	$Ai\varepsilon_\kappa \Sigma_u \frac{K_h E_0(z_a)}{K_a E_0(z_h)}$	$\frac{-i\omega m}{ck_w} \frac{1}{K_a} E_0(z_a)$
2	q_r	$-(\gamma - 1)i\varepsilon_\kappa(1 - i\varepsilon_\kappa)$	$-Ai\varepsilon_\kappa \Sigma_q \frac{K_h E_0(z_a)}{K_a E_0(z_h)}$	—
3	w_θ	—	—	$\frac{i\omega m}{ck_w} \frac{1}{K_a} E_0(z_a)$
4	Total	$1 - i\varepsilon_L - (\gamma - 1)i\varepsilon_\kappa$	$A\varepsilon_\kappa(\varepsilon_\kappa - \varepsilon_L) \frac{K_h E_0(z_a)}{K_a E_0(z_h)}$	0

contribution from either of the non-acoustic modes to the projected sound field.

Corresponding coefficients for the interior region $r < r_0$ are given by replacing $E_0(\xi)$ in Eq. (84) with $F_0(\xi) = J_0(\xi)/J'_0(\xi)$. As mentioned above, acoustic resonances in the interior space cause $F_0(z_a)$ to become large at certain frequencies. Asymptotic analysis yields the $(\Lambda_{ah}, \Lambda_{aw})$ coefficients for $k_0^2 - m^2 = (j'_{0q}/r_0)^2$ as follows. At the first acoustic resonance ($k_0 = m$),

$$(|\Lambda_{ah}|, |\Lambda_{aw}|) \simeq \frac{4}{mr_0} \left(A\varepsilon_\kappa^{1/2}, \varepsilon_\mu^{1/2} \right) \varepsilon_a^{-2}, \tag{93}$$

and at the subsequent transverse-mode resonances

$$(|\Lambda_{ah}|, |\Lambda_{aw}|) \simeq \frac{2}{k_0 r_0} \left(A\varepsilon_\kappa^{1/2}, \frac{m}{k_0} \varepsilon_\mu^{1/2} \right) \varepsilon_a^{-1}, \tag{94}$$

where $\varepsilon_\mu = \omega\mu/\rho c^2$ and $\varepsilon_a = \varepsilon_L + (\gamma - 1)\varepsilon_\kappa$ is the parameter that governs thermoviscous attenuation of the acoustic mode. Such large resonant values invalidate the use of the $\Delta = O(\varepsilon)$ approximation for projecting the acoustic mode into the interior domain at frequencies close to resonance.

E. Cross-modal contamination as a source of error

Although in theory neither the entropy mode nor the vorticity mode can contribute to the projected acoustic field, Table V shows that this depends on the cancellation of potentially large terms. Thus, the u_r and q_r contributions from the entropy mode should cancel³; but any errors in the surface data will lead to errors in the Λ_{ah} terms in rows 1 and 2, potentially destroying their cancellation and causing contamination of the acoustic field. Likewise, the u_r and w_θ contributions from the vorticity mode should cancel in theory, but contamination will occur if the u_r and w_θ data contains errors.

In the parameter space of $(k_0 r_0, |m|/k_0)$ there appear to be no regions where large cancelling terms arise in Λ_{ah} or Λ_{aw} for the exterior radiation problem; the relevant entries in Table V are all $O(\varepsilon^{1/2})$. For interior radiation, the issue of resonances has already been mentioned. The only other

problem for interior radiation occurs with the entropy mode terms when r_0 is much less than the thermal penetration depth l_h , so that $|z_h| \ll 1$. In this (perhaps unlikely) case, the individual Λ_{ah} terms are $O(1)$ and thus are comparable with the sum of the Λ_{aa} terms that represent the acoustic field.

We conclude that when all three modes are present at $r=r_0$ with similar amplitudes $|C_i|$, the generalized Kirchhoff–Helmholtz representation of Sec. III can safely be used for the exterior free-field radiation problem where acoustic waves are extrapolated into $r > r_0$. However, significant problems can arise for acoustic wave projection into interior spaces at frequencies close to acoustic resonance.

VIII. CONCLUSIONS

- (1) The linearly excited sound field in an initially quiescent source-free region \mathcal{V} filled with viscous heat-conducting fluid is determined by the values of $\mathbf{u} \cdot \hat{\mathbf{n}}$, $\mathbf{q} \cdot \hat{\mathbf{n}}$, and $\boldsymbol{\omega} \times \hat{\mathbf{n}}$ on the region’s boundary, together with the fluid properties (ρ, c, c_p, α) and the transport properties (κ, μ, μ_L) , provided \mathcal{V} contains no volume sources.
- (2) The presence in \mathcal{V} of an applied body force $\mathbf{g}(\mathbf{x}, t)$ per unit mass of fluid causes local linear excitation of both the acoustic and entropy modes provided $\text{div } \mathbf{g} \neq 0$. If $\text{curl } \mathbf{g} \neq 0$, the vorticity mode is also excited.
- (3) The presence in \mathcal{V} of a heat input $\sigma(\mathbf{x}, t)$ per unit volume causes local linear excitation of both the acoustic and entropy modes, but not the vorticity mode.
- (4) Explicit time-domain equations for the generalized acoustic variable $\Psi(\mathbf{x}, t)$ and the entropy-mode variable $\Phi(\mathbf{x}, t)$ in an unbounded region, driven by the volume sources (σ, \mathbf{g}) , are summarized in Table I. We present asymptotic approximations accurate to different orders, based on the order parameters $\chi/\bar{\tau}c^2 \ll 1$ and (optionally) $\mu_L/\bar{\tau}\rho c^2 \ll 1$
- (5) Explicit time-domain equations for $\Psi(\mathbf{x}, t)$ and $\Phi(\mathbf{x}, t)$, in a bounded region \mathcal{V} driven by volume sources (σ, \mathbf{g}) and by the boundary data specified in 1. above, are summarized in Table II. As in Table I, different levels of asymptotic approximation are shown.

- (6) The equations in Table II, combined with an appropriate Green’s function, yield solutions for the sound field that generalize the ideal-fluid Kirchhoff–Helmholtz integral to viscous fluids with heat conduction.
- (7) The viscous-dipole boundary-source term in the acoustic mode equation of row 3 is exactly equivalent to the corresponding term in the free-field solution Eq. (10–6.7) of Pierce (1994), as follows from the scalar triple product rule.
- (8) For free-field acoustic radiation problems, whose boundary $\partial\mathcal{V}$ consists of the surface at infinity plus an active boundary \bar{S} , the sound field in \mathcal{V} can be determined in principle from a knowledge of $\mathbf{u} \cdot \hat{\mathbf{n}}$, $\mathbf{q} \cdot \hat{\mathbf{n}}$, and $\boldsymbol{\omega} \times \hat{\mathbf{n}}$ on \bar{S} by using an acoustic Green’s function whose normal derivative vanishes on \bar{S} . This procedure is shown in Sec. VII to be robust, even when all three modes are present on \bar{S} and have comparable dimensionless amplitudes.

The theory presented here can be extended to cover either relaxing gases or elastic solids, although these extensions have not been included for reasons of space.

ACKNOWLEDGMENTS

The authors thank Gwénaél Gabard for valuable assistance in the early stages of this work and Nicolas Joly for confirming the Trilling (1955) generalization, Eq. (75).

APPENDIX A: POLARIZATION/DISPERSION RELATIONS AT HIGHER ORDER

The frequency-domain polarization coefficients (λ_a, λ_h) that allow one to describe the acoustic and entropy modes in terms of P and S are summarized here for thermoviscous fluids, together with the corresponding dispersion relations for each mode.

1. Higher-order polarization relations for thermoviscous fluids

The frequency-domain polarization coefficients (λ_a, λ_h) are defined by

$$S_a = \lambda_a P_a, \quad P_h = \lambda_h S_h. \tag{A1}$$

Values of (λ_a, λ_h) for general thermoviscous fluids are listed below as series expansions in $(-i\epsilon_L, -i\epsilon_L)$. Two types of expansion are given: (i) for $\epsilon_\kappa \ll 1$ with ϵ_L unrestricted and (ii) for $\epsilon = \max(\epsilon_\kappa, \epsilon_L) \ll 1$. In case (i), terms up to $O(\epsilon_\kappa^2)$ are included and in case (ii), terms up to $O(\epsilon^2)$.

Case (i): arbitrary ϵ_L ; $\epsilon_\kappa \ll 1$,

$$\lambda_a = B \left\{ \frac{-i\epsilon_\kappa}{1 - i\epsilon_L} - \epsilon_\kappa^2 \frac{(2 - \gamma - i\epsilon_L)}{(1 - i\epsilon_L)^3} \right\} + O(\epsilon_\kappa^3), \tag{A2}$$

$$\lambda_h = A \left\{ \frac{-i\epsilon_\kappa}{1 - i\epsilon_L} - \frac{(1 - \gamma i\epsilon_L)}{(1 - i\epsilon_L)^3} \left[i\epsilon_\kappa + \epsilon_\kappa^2 \frac{(2 - \gamma - i\epsilon_L)}{(1 - i\epsilon_L)^2} \right] \right\} + O(\epsilon_\kappa^3). \tag{A3}$$

Case (ii): $\epsilon = \max(\epsilon_\kappa, \epsilon_L) \ll 1$,

$$\lambda_a = -i\epsilon_\kappa B J + O(\epsilon^3), \quad \lambda_h = -i(\epsilon_L - \epsilon_\kappa) A J + O(\epsilon^3), \tag{A4}$$

$$J(\epsilon_\kappa, \epsilon_L) = 1 + i\epsilon_L - (2 - \gamma)i\epsilon_\kappa. \tag{A5}$$

2. Dispersion relations for thermoviscous fluids

A similar expansion of the dispersion relations for each mode, keeping the same relative accuracy as above, yields

Case (i): arbitrary ϵ_L ; $\epsilon_\kappa \ll 1$,

$$X_a^{-1} = 1 - i\epsilon_L - \frac{(\gamma - 1)}{1 - i\epsilon_L} i\epsilon_\kappa + \frac{(\gamma - 1)(1 - \gamma i\epsilon_L)}{(1 - i\epsilon_L)^3} \epsilon_\kappa^2 + O(\epsilon_\kappa^3), \tag{A6}$$

$$k_a^2 = \frac{\omega^2}{c^2} \left\{ \frac{1}{1 - i\epsilon_L} + \frac{(\gamma - 1)}{(1 - i\epsilon_L)^3} i\epsilon_\kappa + \frac{(\gamma - 1)}{(1 - i\epsilon_L)^5} \times [2 - \gamma(1 + i\epsilon_L)] \epsilon_\kappa^2 + O(\epsilon_\kappa^3) \right\}, \tag{A7}$$

$$X_h^{-1} = \frac{\gamma i\epsilon_L - 1}{1 - i\epsilon_L} i\epsilon_\kappa - \frac{(\gamma - 1)(1 + \gamma i\epsilon_L)}{(1 - i\epsilon_L)^3} \epsilon_\kappa^2 + O(\epsilon_\kappa^3), \tag{A8}$$

$$k_h^2 = \frac{i\omega}{\chi} \left[\frac{1 - i\epsilon_L}{1 - \gamma i\epsilon_L} - \frac{(\gamma - 1)}{(1 - i\epsilon_L)(1 - \gamma i\epsilon_L)} i\epsilon_\kappa - \frac{(\gamma - 1)}{(1 - i\epsilon_L)^3} \epsilon_\kappa^2 + O(\epsilon_\kappa^3) \right]. \tag{A9}$$

Case (ii): $\epsilon = \max(\epsilon_\kappa, \epsilon_L) \ll 1$,

$$X_a^{-1} = 1 - i\epsilon_L - (\gamma - 1)i\epsilon_\kappa + (\gamma - 1)\epsilon_L \epsilon_\kappa - (\gamma - 1)\epsilon_\kappa^2 + O(\epsilon^3), \tag{A10}$$

$$k_a^2 = \frac{\omega^2}{c^2} \left\{ 1 + i\epsilon_L + (\gamma - 1)i\epsilon_\kappa - [\epsilon_L^2 + (\gamma - 1)(\gamma - 2)\epsilon_\kappa^2 + 3(\gamma - 1)\epsilon_L \epsilon_\kappa] + O(\epsilon^3) \right\}, \tag{A11}$$

$$X_h^{-1} = -i\epsilon_\kappa - (\gamma - 1)\epsilon_L \epsilon_\kappa + (\gamma - 1)\epsilon_\kappa^2 + O(\epsilon^3), \tag{A12}$$

$$k_h^2 = \frac{i\omega}{\chi} \left\{ 1 + (\gamma - 1)i(\epsilon_L - \epsilon_\kappa)[1 + i(\gamma\epsilon_L - \epsilon_\kappa)] + O(\epsilon^3) \right\}. \tag{A13}$$

Relations similar to Eqs. (A11) and (A13) have been given by Cutanda-Henrriquez and Juhl (2013); their Eqs. (A1) and (A2) in our notation are

$$k_a^2 \simeq \frac{\omega^2}{c^2} \left\{ 1 - i\epsilon_L - (\gamma - 1)i\epsilon_\kappa - (\gamma - 1)(\epsilon_\kappa^2 - \epsilon_L \epsilon_\kappa) \right\}^{-1}, \tag{A14}$$

$$k_h^2 = \frac{i\omega}{\chi} \left\{ 1 - (\gamma - 1)i(\epsilon_L - \epsilon_\kappa) \right\}^{-1}. \tag{A15}$$

Series expansion of Eqs. (A14) and (A15) allows comparison with Eqs. (A11) and (A13) and shows the eigenvalues agreeing up to and including $O(\varepsilon^2)$ terms for the acoustic mode. However, agreement extends only to $O(\varepsilon)$ for the entropy mode, meaning the relative error in k_h is $O(\varepsilon^2)$ if one uses Eq. (A15).

APPENDIX B: RESTRICTIONS ON THE VALIDITY OF APPROXIMATE MODE EQUATIONS

In deriving the equations for the acoustic and entropy modes presented in Table I, it was assumed that both modes were excited with comparable amplitudes, so that $\Psi \sim \Phi$ and thus, in regions with no volume sources, $P_a \sim S_h$. In what follows we relax that assumption and instead consider two possible alternative scenarios, to see how far the asymptotic thermoviscous-fluid equations remain valid. In both cases we assume $Y = O(1)$, where $Y = \tilde{\varepsilon}_L/\tilde{\varepsilon}_\kappa$ is the longitudinal Prandtl number,

(a) $P_a \sim \tilde{\varepsilon}_\kappa^n S_h$
 ($n > 0$; the entropy mode dominates locally), (B1)

(b) $S_h \sim \tilde{\varepsilon}_\kappa^q P_a$
 ($q > 0$; the acoustic mode dominates locally). (B2)

For thermal excitation uniformly applied over a plane rigid boundary, with either a prescribed unsteady temperature or an unsteady heat flux, case (a) applies with $n=1/2$; for details see Eq. (75) and Eqs. (44), (45), respectively. If the boundary is adiabatic and either the tangential or normal velocity is prescribed, case (b) applies with $q = 1/2$.

1. Case (a)

The polarization relation $P_h \simeq A(\mathcal{R} - \mathcal{G})S_h$ means that $P_h \sim A\tilde{\varepsilon}S_h$. Combining this with Eq. (B1) leads to

$$P = P_a + P_h = S_h [O(\tilde{\varepsilon}_\kappa^n) + AO(\tilde{\varepsilon})]; \tag{B3}$$

whereas combining the polarization relation $S_a \simeq B\mathcal{G}P_a \sim B\tilde{\varepsilon}_\kappa P_a$ with Eq. (B1) gives

$$S = S_a + S_h = S_h [1 + BO(\tilde{\varepsilon}_\kappa^{n+1})]. \tag{B4}$$

The $\Delta = O(\tilde{\varepsilon})$ version of the acoustic mode equation based on the lossless wave operator, as in row 3 of Table II, has a residual error given by

$$D_a = [\mathcal{R} + (\gamma - 1)\mathcal{G} + O(\tilde{\varepsilon}^2)] \frac{\partial^2 P}{\partial t^2} + A(Y - 1)[\mathcal{R} + (\gamma - 2)\mathcal{G} + O(\tilde{\varepsilon}^2)] \frac{\partial^2 S}{\partial t^2} \tag{B5}$$

$$\sim \tilde{\varepsilon}_\kappa \max \left[(Y + \gamma - 1) \frac{\partial^2 P}{\partial t^2}, A(Y - 1)(Y + \gamma - 2) \frac{\partial^2 S}{\partial t^2} \right]. \tag{B6}$$

Substituting Eqs. (B3) and (B4) in Eq. (B6) shows that for case (a) the residual error is controlled by the entropy mode component of the $\partial^2 S/\partial t^2$ term in Eq. (B6), leading to $D_a \sim A(Y - 1)(Y + \gamma - 2)(\partial^2 S_h/\partial t^2)\tilde{\varepsilon}_\kappa$. Dividing by $\partial^2 P_a/\partial t^2 \sim \tilde{\varepsilon}_\kappa^n \partial^2 S_h/\partial t^2$ then gives the relative error of the acoustic mode equation as

$$\Delta_a \sim (Y - 1)(Y + \gamma - 2)A\tilde{\varepsilon}_\kappa^{1-n}. \tag{B7}$$

Equation (B7) shows that in case (a) the asymptotic accuracy of the acoustic mode equation in row 3 of Table II is reduced from its nominal value of $\Delta = O(\tilde{\varepsilon})$, which was based on the restrictive assumption that $P_a \sim S_h$. However, the approximate equation remains viable as long as $n < 1$.

Using the dissipative wave operator shown in row 3 of Table I leads to a similar conclusion. The residual error becomes

$$D'_a = (Y - 1) \left\{ -(\gamma - 1)\mathcal{G}[\mathcal{R} + (\gamma - 1)\mathcal{G} + O(\tilde{\varepsilon}^2)] \frac{\partial^2 P}{\partial t^2} + A[\mathcal{R} + (\gamma - 2)\mathcal{G} + O(\tilde{\varepsilon}^2)] \frac{\partial^2 S}{\partial t^2} \right\} \tag{B8}$$

$$\sim A(Y - 1)(Y + \gamma - 2) \frac{\partial^2 S_h}{\partial t^2} \tilde{\varepsilon}_\kappa. \tag{B9}$$

This is the same leading term as found previously, so Eq. (B7) remains unaltered. Note that the acoustic mode residuals (D_a, D'_a) discussed above, based on the $\Delta = O(\tilde{\varepsilon})$ equations in rows 3 of Tables II and I, respectively, differ from those previously found in Sec. III C for the $\Delta = O(\tilde{\varepsilon}_\kappa)$ arbitrary- $\tilde{\varepsilon}_L$ equations in rows 1 of each table, even in the limit $\varepsilon_L \ll 1$. This difference is due to the slightly different operators \mathcal{L}_a and acoustic variables Ψ required by the two levels of approximation.

Finally, far from any scattering boundaries or localized source inputs the entropy mode may be neglected entirely because of its exponential decay. The magnitude of the residual term relative to either term on the left of the acoustic mode equation then follows as

$$\Delta_a \sim (Y + \gamma - 1)\tilde{\varepsilon}_\kappa \quad \text{or} \quad \Delta'_a \sim (\gamma - 1)(Y - 1)(Y + \gamma - 1)\tilde{\varepsilon}_\kappa^2, \tag{B10}$$

depending on which of the alternative $\Delta = O(\tilde{\varepsilon})$ equations (Table II or Table I) is adopted.

2. Case (b)

Combining Eq. (B2) with the polarization relation $S_a \simeq B\mathcal{G}P_a \sim B\tilde{\varepsilon}_\kappa P_a$ from Eqs. (A1) and (A4) gives

$$S = S_a + S_h = P_a [B\tilde{\varepsilon}_\kappa + O(\tilde{\varepsilon}_\kappa^q)]; \tag{B11}$$

whereas combining $P_h \sim A\tilde{\varepsilon}S_h$ with Eq. (B2) gives

$$P = P_a + P_h = P_a [1 + A\tilde{\varepsilon}O(\tilde{\varepsilon}_\kappa^q)]. \tag{B12}$$

The entropy mode diffusion equation in row 4 of Table I, labelled $\Delta = O(\tilde{\varepsilon})$, has a residual error whose asymptotic form is shown in Sec. III [Eq. (25)] to be

$$D_h = (\gamma - 1)[\mathcal{R} - \mathcal{G} + O(\tilde{\varepsilon}^2)] \frac{\partial S}{\partial t} + B[\mathcal{G} + O(\tilde{\varepsilon}^2)] \frac{\partial P}{\partial t} \quad (\text{B13})$$

$$\sim \max \left[(\gamma - 1)(Y - 1) \frac{\partial S}{\partial t} \tilde{\varepsilon}_\kappa, B \frac{\partial P}{\partial t} \tilde{\varepsilon}_\kappa \right]. \quad (\text{B14})$$

Substituting Eqs. (B11) and (B12) in Eq. (B14) shows that for case (b) the residual error is controlled by the acoustic mode component of the $\partial P/\partial t$ term in Eq. (B14), leading to $D_h \sim B(\partial P_a/\partial t)\tilde{\varepsilon}_\kappa$. Dividing by $\partial S_h/\partial t \sim \tilde{\varepsilon}_\kappa^q \partial P_a/\partial t$ then gives the relative error of the entropy mode equation as

$$\Delta_h \sim B\tilde{\varepsilon}_\kappa^{1-q}. \quad (\text{B15})$$

Equation (B15) shows that in case (b), the asymptotic accuracy of the entropy mode equations in row 4 of Tables I and II is reduced from the nominal value of $\Delta = O(\tilde{\varepsilon})$, but the approximation remains viable provided $q < 1$.

APPENDIX C: EXACT RELATIONS BETWEEN MODAL POTENTIALS AND FLUID PROPERTY PERTURBATIONS WITH $(\sigma, \mathbf{g})=0$

1. Modal pressure and entropy coefficients

Applying the linearized continuity and momentum equations to the acoustic and entropy modes separately gives, for single-frequency disturbances,

$$k_i^2 \varphi_i = -i\omega(P_i - AS_i), \quad i = (a, h); \quad (\text{C1})$$

$$\frac{i\omega}{c^2} \varphi_i = (1 - i\varepsilon_L)P_i + Ai\varepsilon_L S_i. \quad (\text{C2})$$

We define non-dimensional coefficients for pressure (f_a, f_h), entropy (g_a, g_h) and temperature (h_a, h_h) by writing

$$P_i = f_i \frac{i\omega}{c^2} \varphi_i, \quad S_i = g_i \frac{i\omega}{c^2} \varphi_i, \quad \frac{T'_i}{T_0} = h_i \frac{i\omega}{c^2} \varphi_i, \quad (\text{C3})$$

where $h_i = (Bf_i + g_i)$. It follows from Eqs. (C1) and (C2) that

$$f_i = (1 + i\varepsilon_L X_i), \quad g_i = (1/A)[1 - (1 - i\varepsilon_L)X_i]. \quad (\text{C4})$$

The pressure coefficient f_i above is consistent with Eqs. (A6) and (A7) of Cutanda-Henrriquez and Juhl (2013); their coefficients (ϕ_a, ϕ_h) are related to (f_a, f_h) by

$$\phi_i = (i\omega f_i)^{-1}, \quad (\text{C5})$$

using our notation with $e^{-i\omega t}$ time dependence. Note that the (f_i, g_i) expressions in Eq. (C4) also give the modal polarization coefficients in terms of the X_i , since $P_i/S_i = f_i/g_i$.

2. Alternative form of (f, g, h) coefficients

Alternatively one can combine Eq. (C1) with the entropy equation, which in the absence of heat sources is

TABLE VI. Exact pressure, entropy, and temperature coefficients as defined in Eq. (C3) for the acoustic and entropy modes in a thermoviscous fluid, together with the associated polarization coefficients. Results are expressed in terms of either $(\varepsilon_\kappa, X_i)$ or (ε_L, X_i) , where X_i are the dimensionless squared wavenumbers for the mode.

Coefficient	ε_κ version	ε_L version
f_i	$X_i \frac{1 + i\varepsilon_\kappa X_i}{1 + i\varepsilon_\kappa \gamma X_i}$	$(1 + i\varepsilon_L X_i)$
g_i	$\frac{-i\varepsilon_\kappa B X_i^2}{1 + i\varepsilon_\kappa \gamma X_i}$	$(1/A)[1 - (1 - i\varepsilon_L)X_i]$
h_i	$\frac{B X_i}{1 + i\varepsilon_\kappa \gamma X_i}$	$(1/A)[\gamma - (1 - \gamma i\varepsilon_L)X_i]$
P_i/S_i	$\frac{-(1 + i\varepsilon_\kappa X_i)}{i\varepsilon_\kappa B X_i}$	$A \frac{1 + i\varepsilon_L X_i}{1 - (1 - i\varepsilon_L)X_i}$

$$(\rho T c_p)_0 \frac{\partial S}{\partial t} = \kappa \nabla^2 T, \quad \text{i.e.,} \quad T'_i/T_0 = -(i\varepsilon_\kappa)^{-1} X_i^{-1} S_i \quad (\text{C6})$$

for $e^{-i\omega t}$ time dependence. This leads to versions of the pressure and entropy coefficients (f_i, g_i) that are equivalent to Eq. (C4), but involve ε_κ instead of ε_L . The results are

$$f_i = X_i \frac{1 + i\varepsilon_\kappa X_i}{1 + i\varepsilon_\kappa \gamma X_i}, \quad g_i = \frac{-i\varepsilon_\kappa B X_i^2}{1 + i\varepsilon_\kappa \gamma X_i}. \quad (\text{C7})$$

As a check we can use Eq. (C7) to obtain a relation between T'_i/T_0 and P_i that is equivalent to Eqs. (A4) and (A5) of Cutanda-Henrriquez and Juhl (2013), i.e.,

$$T'_i/T_0 = \frac{B P_i}{1 + i\varepsilon_\kappa X_i}. \quad (\text{C8})$$

3. Summary of results

The modal coefficients (f_i, g_i, h_i) derived above relate the dimensionless fluid-property perturbations ($P_i, S_i, T'_i/T_0$) to φ_i . They are given in Table IV, together with the polarization coefficients they imply. There are two equivalent versions of each coefficient, one involving ε_κ and the other involving ε_L ; both versions are exact.

Although in principle one can use any of ($P_i, S_i, T'_i/T_0$) as primary variables rather than the potentials φ_i , the first option can lead to problems as $Y = \varepsilon_L/\varepsilon_\kappa \rightarrow 1$. In that limiting case the entropy-mode pressure coefficient f_h is zero and Eq. (C8) breaks down, because P_h vanishes.

¹Note that Pierce (1994) uses $s' = c_p S$ and $(\alpha/\rho)p' = \alpha c^2 P = c_p B P$ as variables, rather than S and P .

²The $|\mathbf{u}_a|/c$ interpretation breaks down for case (b) at certain frequencies above cutoff ($k_0 > |m|$), on account of resonances in the interior space.

³The $\Delta = O(\varepsilon)$ asymptotic approximation produces an $O(\varepsilon)$ relative error in the coefficient Λ_{ah} (as might be expected), leading to an $O(\varepsilon^{3/2})$ relative error in \tilde{C}_a for external radiation (under the assumption that all three modes are equally excited).

- Bass, H. E., Sutherland, L. C., and Zuckerwar, A. J. (1990). "Atmospheric absorption of sound: Update," *J. Acoust. Soc. Am.* **88**(4), 2019–2021.
- Beltman, W. M. (1999). "Viscothermal wave propagation including acousto-elastic interaction, Part I: Theory," *J. Sound Vib.* **227**, 555–586.
- Bruneau, M. (2006). *Fundamentals of Acoustics* (ISTE, London).
- Bruneau, M., Herzog, P., Kergomard, J., and Polack, J. D. (1989). "General formulation of the dispersion equation in bounded visco-thermal fluid, and application to some simple geometries," *Wave Motion* **11**, 441–451.
- Chu, B. T., and Kováznay, L. S. G. (1958). "Non-linear interactions in a viscous heat-conducting compressible gas," *J. Fluid Mech.* **3**, 494–514.
- Cutanda-Henríquez, V., and Juhl, P. M. (2013). "An axisymmetric boundary element formulation of sound wave propagation in fluids including viscous and thermal losses," *J. Acoust. Soc. Am.* **134**(5), 3409–3418.
- Deresiewicz, H. (1957). "Plane waves in a thermoelastic solid," *J. Acoust. Soc. Am.* **29**(204), 204–209.
- Greenspan, M. (1950). "Propagation of sound in rarefied helium," *J. Acoust. Soc. Am.* **22**, 568–571.
- Greenspan, M. (1956). "Propagation of sound in five monatomic gases," *J. Acoust. Soc. Am.* **28**, 644–648.
- Greenspan, M. (1959). "Rotational relaxation in nitrogen, oxygen and air," *J. Acoust. Soc. Am.* **31**, 155–160.
- Guiraud, P., Giordano, S., Bou-Matar, O., Pernod, P., and Lardat, R. (2019). "Multilayer modeling of thermoacoustic sound generation for thermophone analysis and design," *J. Sound Vib.* **455**, 275–298.
- Howe, M. S. (1996). *Acoustics of Fluid-Structure Interaction* (Cambridge University Press, Cambridge).
- Jones, D. S. (1986). *Acoustic and Electromagnetic Waves* (Clarendon Press, Oxford), Sec. 1.19.
- Kirchhoff, G. (1868). "Über den Einfluss der Wärmeleitung in einem Gase auf die Schallbewegung" ("On the influence of heat conduction in a gas on sound propagation"), *Ann. Phys. Chem.* **210**, 177–193.
- Kováznay, L. S. G. (1953). "Turbulence in supersonic flow," *J. Aeronaut. Sci.* **20**(10), 657–674.
- Lighthill, M. J. (1978). *Waves in Fluids* (Cambridge University Press, Cambridge).
- McDonald, F. A., and Wetsel, G. C., Jr. (1978). "Generalized theory of the photoacoustic effect," *J. Appl. Phys.* **49**(4), 2313–2322.
- Morfeý, C. L., Sorokin, S. V., and Gabard, G. (2012). "The effects of viscosity on sound radiation near solid surfaces," *J. Fluid Mech.* **690**, 441–460.
- Morse, P. M., and Ingård, K. U. (1968). *Theoretical Acoustics* (McGraw-Hill, New York).
- Pierce, A. D. (1985). "The inhomogeneous wave equation of thermoacoustics," in *Flow of Real Fluids* (Springer Verlag, Berlin), pp. 92–100.
- Pierce, A. D. (1994). *Acoustics: An Introduction to Its Physical Principles and Applications*, 3rd ed., reissued 2019 (Acoustical Society of America, Melville, NY).
- Rayleigh, L. (1894). *Theory of Sound Vol. II*, 2nd ed. (Macmillan, London).
- Temkin, S. (1981). *Elements of Acoustics* (John Wiley, New York).
- Trilling, L. (1955). "On thermally induced sound fields," *J. Acoust. Soc. Am.* **27**(3), 425–431.